

2000

Assessing the classification accuracy of digitized National Aerial Photography Program imagery: Comparison with botanical data

Mark Arthur Alexander
University of Northern Iowa

Let us know how access to this document benefits you

Copyright ©2000 Mark Arthur Alexander

Follow this and additional works at: <https://scholarworks.uni.edu/etd>



Part of the [Remote Sensing Commons](#)

Recommended Citation

Alexander, Mark Arthur, "Assessing the classification accuracy of digitized National Aerial Photography Program imagery: Comparison with botanical data" (2000). *Dissertations and Theses @ UNI*. 619.

<https://scholarworks.uni.edu/etd/619>

This Open Access Thesis is brought to you for free and open access by the Student Work at UNI ScholarWorks. It has been accepted for inclusion in Dissertations and Theses @ UNI by an authorized administrator of UNI ScholarWorks. For more information, please contact scholarworks@uni.edu.

Offensive Materials Statement: Materials located in UNI ScholarWorks come from a broad range of sources and time periods. Some of these materials may contain offensive stereotypes, ideas, visuals, or language.

ASSESSING THE CLASSIFICATION ACCURACY OF DIGITIZED
NATIONAL AERIAL PHOTOGRAPHY PROGRAM IMAGERY:
COMPARISON WITH BOTANICAL DATA

An Abstract of a Thesis
Submitted
In Partial Fulfillment
Of the Requirements for the Degree
Master of Arts

Mark Arthur Alexander
University of Northern Iowa
May 2000

ABSTRACT

The ability to acquire and use remotely sensed data has revolutionized large-scale ecological studies by reducing dependence on difficult and expensive field survey techniques for acquisition of land use and land cover data. Multispectral satellite imagery, typically from the Landsat Multispectral Scanner (MSS), Thematic Mapper (TM) and the SPOT High Resolution Visible (HRV) instruments, has proven particularly valuable in surveying and classifying vegetation cover (Frank & Thorn, 1985). Further studies have concluded that alpine vegetation communities and habitats can be mapped successfully by including the geomorphic parameters of elevation, slope, and incidence when classifying remotely sensed data.

This research analyzes the degree of classification accuracy that can be obtained by using digitized National Aerial Photography Program (NAPP) aerial photographs and topographic data derived from a digital elevation model (DEM) by comparing these to detailed tundra vegetation and topographic data for an alpine tundra area in the Wind River Range, Wyoming.

Two main objectives are associated with this research. The first objective is to determine the extent to which alpine vegetation types are visible with the spatial and spectral characteristics of digitized NAPP imagery. The second objective is to determine if topographic information such as elevation, slope, and aspect data derived from manual field study and a USGS DEM will increase the overall classification accuracy when combined with the digital color channels of the digitized NAPP.

Discriminant function analysis was used to conduct the statistical classifications of the data sets. Bivariate relationships among the field and digitized NAPP variables were evaluated to test for variable similarity and to aid in the prediction of what kind of results can be expected from discriminant function classification. Statistical classification using linear discriminant analysis produced overall classification accuracies of 76.17% for the spectral data (digitized NAPP RGB). The classification accuracy of the integrated digitized NAPP and DEM data sets was 84.38%. This is significantly greater than the classification of either data set alone. These results support the idea reported in the literature, it is necessary to integrated TM and DEM data in multispectral classifications of mountain environments.

ASSESSING THE CLASSIFICATION ACCURACY OF DIGITIZED
NATIONAL AERIAL PHOTOGRAPHY PROGRAM IMAGERY:
COMPARISON WITH BOTANICAL DATA

A Thesis

Submitted

In Partial Fulfillment

Of the Requirements for the Degree

Master of Arts

Mark Arthur Alexander

University of Northern Iowa

May 2000

This Study by: Mark Arthur Alexander

Entitled: ASSESSING THE CLASSIFICATION ACCURACY OF
DIGITIZED NATIONAL AERIAL PHOTOGRAPHY PROGRAM
IMAGERY: COMPARISON WITH BOTANICAL DATA

has been approved as meeting the thesis requirement for the
Degree of Master of Arts

4.13.00
Date _____
Dr. Dennis E. Dahms, Chair, Thesis Committee

04/13/00
Date _____
Dr. Michael E. Emch, Thesis Committee

4/13/2000
Date _____
Dr. James C. Walters, Thesis Committee

6/8/2000
Date _____
Dr. John W. Somervill, Dean, Graduate College

DEDICATION

I would like to dedicate this research to my wife, Michelle, who provided unwavering patience and support throughout my education and thesis research.

ACKNOWLEDGMENTS

I would like to express sincere gratitude to Dr. Dennis E. Dahms, for his insight, support and providing me the freedom and opportunity to grow as a student.

I would also like to thank Dr. Michael E. Emch for his sound technical advice and support.

Special thanks to Dr. James C. Walters for providing quality instruction and valuable knowledge to my research.

I would also like to express sincere thanks to Biologist Dr. Richard W. Scott of Central Wyoming College for providing me access to his vegetation data and for taking the time from a busy schedule to answer questions and provide information when needed.

Great appreciation to James R. Dickerson for invaluable insight and advice throughout this research.

I would also like to thank David Hartley for his help and providing access to the necessary equipment to accomplish this research.

TABLE OF CONTENTS

	PAGE
LIST OF TABLES	vii
LIST OF FIGURES	viii
CHAPTER 1. INTRODUCTION	1
Research Objectives	4
Study Area	5
Regional Geology	5
Roaring Fork Mountain	5
CHAPTER 2. LITERATURE REVIEW	10
Previous High Mountain Ecosystems Investigations	10
Mountain Environments	12
Synthetic Alpine Slope	15
Alpine Vegetation Classes	17
Remote Sensing Investigations	19
Aerial Photography and Multispectral Investigations	19
Classification and Accuracy Assessment Investigations	24
CHAPTER 3. METHODOLOGY	27
Global Positioning System Data Collection	28
Field Data	29

	PAGE
Integrating the NAPP Imagery	35
Digitizing the NAPP Imagery	37
Image Processing	39
Orthorectification	43
DEM Data	46
Classification of Digitized NAPP Imagery and DEM Data	50
CHAPTER 4. ANALYSIS AND RESULTS	55
Signature Evaluation	56
Transformed Divergence	56
Cospectral Feature Space Plots	64
Bivariate Correlation	68
Discriminant Analysis Classification and Accuracy Assessment	74
Digitized NAPP Error Matrix	75
Evaluating Field and DEM Topographic Data	79
Evaluation of Digitized NAPP and DEM Topographic Data	81
Integrated Digitized NAPP and DEM Error Matrix	84
CHAPTER 5. CONCLUSIONS	87
Summary and Recommendations for Future Research	88
REFERENCES	91
APPENDIX A: NATIONAL AERIAL PHOTOGRAPHY PROGRAM	99
APPENDIX B: SUPERVISED CLASSIFICATION MAP	101

LIST OF TABLES

TABLE	PAGE
1 Comparison of Available Sensors for Project	4
2 Alpine Tundra Plant Communities	12
3 Classification Scheme of Alpine Plant-Growth Forms	18
4 Alpine Vegetation Classes	21
5 Casper GPS Community Base Station (CBS)	29
6 Roaring Fork Mountain Global Positioning System Data Collection August 8, 1998	30
7 Roaring Fork Mountain Global Positioning System Data Collection August 9, 1998	30
8 Roaring Fork Mountain Ground Control Point Global Positioning System Data Collection August 9, 1998	31
9 Dr. Richard Scott's Topographic Data for Alpine Vegetation Located on Roaring Fork Mountain, Wyoming	32
10 Classification System and Number of Training Samples/Pixels	35
11 Computation of Pixel Ground Resolution	38
12 Signature Separability Listing Using Bands: 1 2 3 Taken 3 at a Time	58
13 Signature Separability Listing Using Bands: 1 2 3 Taken 2 at a Time	59
14 Signature Separability Listing Using Bands: 1 2 3 Taken 1 at a Time	60
15 Bivariate Correlations	69
16 Error Matrix of the Classification Map of Roaring Fork Mountain, Wyoming Derived from Digitized NAPP Data	77
17 Summary of Classification Accuracies of the Field and DEM Topographic Variables are Percent Accuracy by Class	80

TABLE	PAGE
18 Summary of Classification Accuracies of the Digitized NAPP channels 1-3 and DEM Data Set	82
19 Error Matrix of the Classification Map Derived from Digitized NAPP Data of Roaring Fork Mountain, Wyoming Combined with DEM Data	85
20 NAPP Parameters.....	100

LIST OF FIGURES

FIGURE	PAGE
1 Wind River Range, Wyoming. Study site located east of Stough Creek Basin on Roaring Fork Mountain	6
2 Image inset shows the “horseshoe” of Roaring Fork Mountain. The smaller inset describes the portion of Roaring Fork Mountain used for this study. Insets show Roaring Fork Mountain and Study area. Digitized NAPP image 1778-08 August, 06 1992. Scale 1:40000	8
3 Synthetic Alpine Slope Model: Microenvironmental sites on the leeward side of the slope as described by Burns (1980) and Burns and Tonkin (1982).....	16
4 Vegetation sites selected by Scott and subsequently revisited and geolocated using GPS	34
5 Spectral Sensitivity Color infrared films are sensitive to ultraviolet, visible, and infrared radiation to approximately 900 nm	36
6 Illustrates data volume increases geometrically as the micrometer is decreased...	39
7 Histogram and image are prior to the application of the histogram equalization	41
8 Histogram and image after application of the histogram equalization	42
9 Illustrates the Orthorectification Model used to rectify the Digitized NAPP to three dimensions	44
10 Orthorectified color composite scene of the RGB Bands 1, 2, 3 of the study area	45
11 Elevation image of the study area. Scale approximately 1:18000	47
12 Slope image of the study area. Scale approximately 1:18000	48
13 Aspect Image of the study area. Scale approximately 1:18000	49

FIGURE	PAGE
14 Plot of the Roaring Fork Mountain, Wyoming, digitized NAPP training statistics for five classes measured in Bands 1 and 3 displayed as co-spectral parallelepiped. The upper and lower limit of each parallelepiped is ± 1 standard deviation	65
15 Plot of the Roaring Fork Mountain, Wyoming, digitized NAPP training statistics for five classes measured in Bands 1 and 2 displayed as co-spectral parallelepiped. The upper and lower limit of each parallelepiped is ± 1 standard deviation	66
16 Plot of the Roaring Fork Mountain, Wyoming, digitized NAPP training statistics for five classes measured in Bands 2 and 3 displayed as co-spectral parallelepiped. The upper and lower limit of each parallelepiped is ± 1 standard deviation	67

CHAPTER 1

INTRODUCTION

The ability to acquire and use remotely sensed data has revolutionized large-scale ecological studies by reducing dependence on difficult and expensive field survey techniques for acquisition of land use and land cover data. Multispectral satellite imagery, typically from the Landsat Multispectral Scanner (MSS), Thematic Mapper (TM) and the SPOT High Resolution Visible (HRV) instruments, has proven particularly valuable in surveying and classifying vegetation cover (Frank & Thorn, 1985). However, studies of alpine landscapes in western North America using remotely-sensed imagery to map vegetation distribution show relatively low levels of classification success (Fleming, 1988; Harvie, Cihlar, & Goodfellow, 1982; Kenk, Sondheim & Yee, 1988; Markon, 1992). Studies in normally accessible areas such as agricultural regions and forests often can rely on “ground truthed” data in the form of vegetation maps to which aerial and/or satellite imagery can be compared for improved accuracy classification (Jennings, 1996). In the relatively inaccessible terrain of alpine tundra ecosystems, ground inventory and assessment is difficult, time consuming, expensive, and often inaccurate (Frank & Thorn, 1985). Thus, ground accuracy, similar to that available in more accessible areas, is usually not possible in mountain areas. Remotely sensed imagery often is the only data source available for vegetation mapping in such inaccessible areas (Crist & Deitner, 1998). Mapping of such an area can be achieved economically only with the aid of large-scale aerial color infrared photography (Jensen, 1996).

Terrain classification is the grouping of earth surface regions that are similar in certain attributes including vegetation, soils and geomorphic characteristic. This method of classification traditionally is accomplished by remote sensors such as Landsats earlier Multispectral Scanners (MSS), Thematic Mapper (TM) and the more recent Landsat Enhanced Thematic Mapper (ETM+). Classification of remotely sensed imagery involves the creation of rules based on the unique spectral signatures of the different land cover types. The success of each classification depends on the ability of the sensor to detect the terrain attributes of interest (Jensen, 1996). In low relief areas, land cover attributes are well represented by the spectral and spatial response of the Landsat sensor. In high relief areas however, mapping accuracy suffers in several ways when using only remotely sensed imagery: (a) classification accuracy may decrease because of topographic effects (Holben & Justice, 1981) and the large degree of topographic and geomorphic variability over relatively small areas in alpine regions (Frank, 1988), and (b) the lower spatial resolution of traditional imagery such as Landsat and SPOT reduce the classification accuracy. Consequently, there is increased interest in combining, high spatial, accurate up-to-date remotely-sensed data and ancillary data such as slope, aspect and digital elevation models. Such combinations of data may enhance land cover classification for the ultimate use in the study of ecosystem change.

Alpine regions have been studied and mapped in the past for several reasons: (a) inventory of vegetation species and patterns (Bamberg, 1961; Billings, 1988; Scott, 1995; Walsh, Bian, Brown, Butler, & Malanson, 1989), (b) geomorphic activity (Billings, 1988; Caine, 1969), (c) land use planning (Ives & Bovis, 1978), and (d) association with

geologic features (Butler & Walsh 1990; Gardner, 1986; Walsh, Cooper, Van Essen, & Gallagher, 1990). The mapping in these alpine regions was accomplished using a combination of traditional field techniques. In more recent studies traditional techniques were used to guide automated digital classification from remotely sensed imagery (Billings, 1988; Butler & Walsh, 1990). It can be concluded from these studies, that specific vegetation communities and habitats can be mapped successfully by including the geomorphic parameters of elevation, slope, and incidence when classifying remotely sensed data. My research seeks an economical method that scientists can use to find and monitor alpine vegetation. I will analyze the degree of classification accuracy that can be obtained by using digitized National Aerial Photography Program (NAPP) aerial photographs and topographic data derived from a digital elevation model (DEM) by comparing these to detailed tundra community vegetation and topographic data for an alpine tundra area in the Wind River Range, Wyoming.

Selection of remotely sensed data used here are based on criteria set by Jensen (1996). The considerations used in the selection are spectral, temporal, and radiometric resolution. I added cost to this set of criteria in order to develop an economical technique that uses remotely sensed data as a reconnaissance tool for the classification of alpine vegetation. NAPP imagery was chosen over other forms of imagery for several reasons: (a) it captures data in both visible and NIR wavelengths, (b) it has the ability to contain high digitized geometric resolution, (c) it is readily available for the study area, and (d) the total cost of acquiring the data is low. These parameters are compared to those of other sensors in Table 1.

Table 1

Comparison of Available Sensors for Project

Sensor	Resolution in (Multispectral)	Cost
Landsat 5 TM (Last 10 Years)	30 x 30 Meter	\$2500-4000
Landsat 7 ETM+	30 x 30 Meter	\$600
SPOT XS, XI	20 x 20 Meter	\$2500
NAPP Digitized at 25 Micrometers	1 Meter	\$30

Research Objectives

Two main objectives are associated with this research. The first objective is to determine the extent to which alpine vegetation types are visible with the spatial and spectral characteristics of digitized NAPP imagery. The second objective is to determine if topographic information such as elevation, slope, and aspect data derived from manual field study and a USGS DEM will increase the overall classification accuracy when combined with the digital color channels of the digitized NAPP.

Related to the major objectives are a number of secondary objectives: (a) to determine classification accuracies of the spectral and integrated data sets, (b) to confirm an improvement in classification accuracy by adding the DEM data to the spectral data set, and (c) to determine whether the derived technique using digitized NAPP and DEM data can be used to classify alpine vegetation beyond this study area.

A result of this project will be to demonstrate the scale at which digital NAPP imagery can reproduce traditional ground-based mapping. A demonstration of this scale is critical for future vegetation mapping of wilderness ecosystems, especially in alpine regions where, as mentioned previously, ground logistics are limited, and traditional mapping techniques are difficult or too expensive.

Study Area

Regional Geology

The Wind River Range is the largest mountain chain in Wyoming (Figure 1). The range trends NW/SE approximately 140 miles from Terrace Mountain in the north to South Pass City (Blackstone, 1993). Forty-seven of the 50 peaks in Wyoming over 4000 meters in elevation are found in the Wind River Range (Steidtmann, Middleton, & Shuster, 1989). The topographic crest of the range, including the state's highest point, Gannett Peak, forms over 100 miles of the continental Divide (Blackstone, 1993).

The Wind River Range is an eroded, double-plunging, asymmetrical anticline that was raised 60-40 million years ago during the late Cretaceous-early Eocene Laramide orogeny. The main massif of the range primarily consists of 3.4 and 2.3 billion year old Precambrian granodiorite plutons with smaller areas of migmatite, gneiss, and meta-sedimentary rocks (Blackstone, 1993).

Roaring Fork Mountain

The 286.9 hectare study site is located on eastern flank of Roaring Fork Mountain approximately 32 km southwest of Lander, Wyoming (Figure 2). Roaring Fork Mountain is composed mainly of granite of the Louis Lake Formation (Snook et al., 1996) which



Figure 1. Wind River Range, Wyoming. Study site located just east of Stough Creek Basin on Roaring Fork Mountain.

has been intruded locally by a number of mafic dikes. Roaring Fork Mountain is essentially an extensive summit flat that is a remnant of the regional surface that existed prior to the uplift of the range during the Laramide Orogeny (Blackstone, 1993).

Gently sloped summits and ridges (collectively referred to as summit flats) are abundant in many Laramide ranges in the western United States (Small & Anderson, 1998). As with any environment, the most important geologic factors in the production of the landscape are lithology and structure. These have an influence in that they tend to control the response of a landform through the resistance and strength of its constituent material (Caine, 1969). Summit flat environments, such as the alpine landscapes of Roaring Fork Mountain, are notable for the variability of their erosional resistance (Small & Anderson, 1998). Geologic, physiographic, climatic, hydrologic, and biotic factors, as well as mechanical and chemical weathering are a few of the characteristics and processes responsible for influencing erosional change in alpine environments. Generally, the alpine environment is normally characterized by a high rate of energy transfer and this is particularly evident where steep slopes prevail (Caine, 1969). However, steep gradients are not as prevalent in summit flat environments so erosion rates and accumulation of waste is less rapid (Small & Anderson, 1998).

Thus, these alpine environments support diverse ecosystems with extensive vegetation communities that change noticeably over short distances with local geomorphic variations. The present surface of the eastern flank of Roaring Fork Mountain ranges from 2800 to 3500 m in elevation and is essentially fellfield with

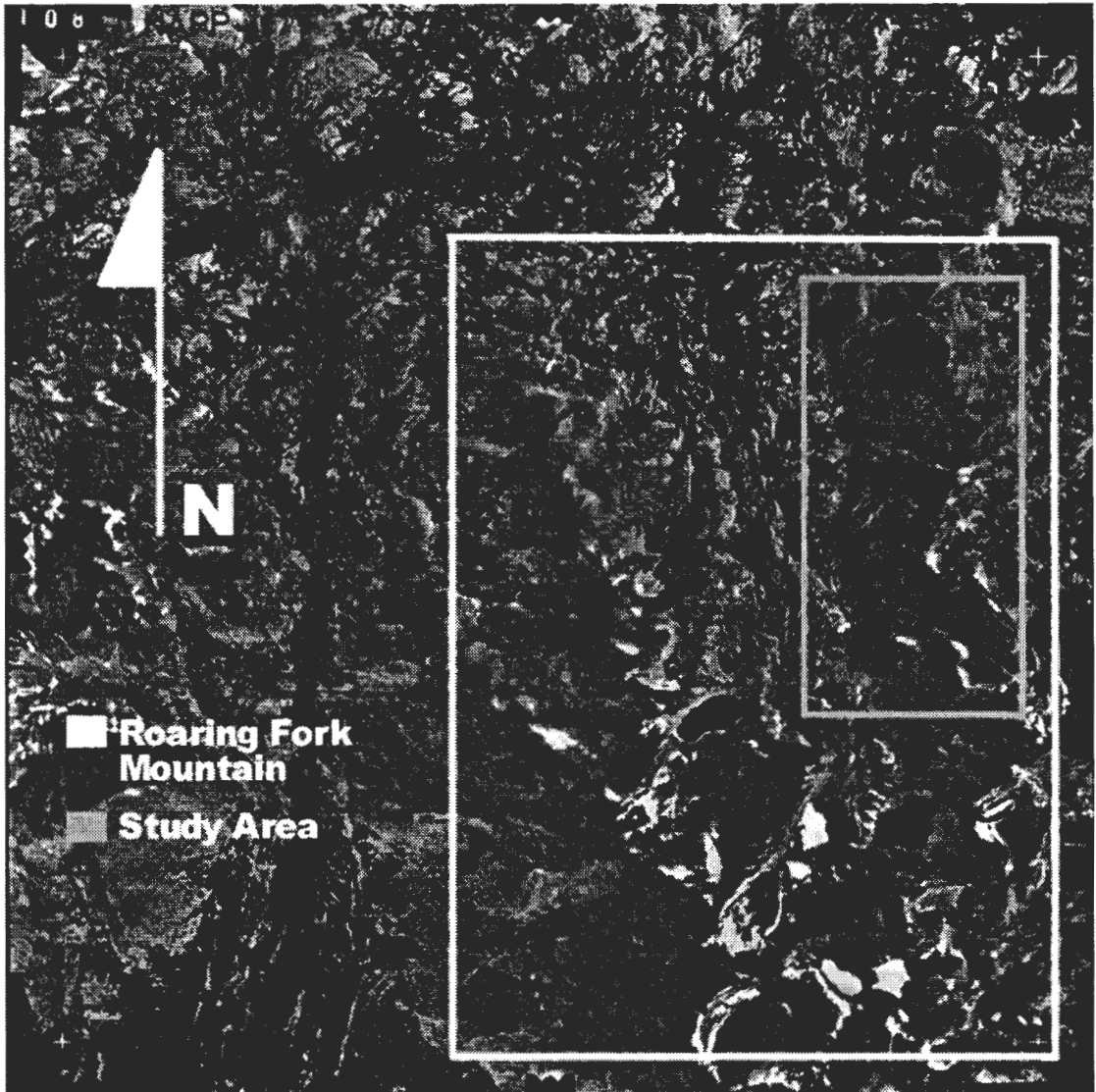


Figure 2. Image inset shows the “horseshoe” of Roaring Fork Mountain. The smaller inset describes the portion of Roaring Fork Mountain used for this study. Insets show Roaring Fork Mountain and study area. Digitized NAPP image 1778-08 August, 06 1992. Scale 1:40000.

patches of felsenmeer (Scott, 1998). The vegetation on Roaring Fork Mountain generally consists of alpine tundra communities with low willow stands in favorable moist places.

Turf is found on both slopes and level sites and small sedge and grass "meadows" are scattered throughout the area. Also, semi-barren ridge tops are present with late snow-melt areas. Snow accumulation and availability of water are apparently the primary controls on species composition (R.W. Scott, personal communication, April 12, 1998).

Climate on Roaring Fork Mountain is typical of mid-latitude alpine environments. During a 122-day sampling period in the summer of 1992 (June-October) two microclimate stations located on Roaring Fork Mountain at an elevation of 3383 m recorded average summer air temperature conditions 5-9 degrees C at the alpine vegetation-atmosphere boundary; 10 cm or less above the ground surface. Daily maximum ranged from 10-16 degrees C while daily minimums averaged 0-3 (Scott, 1995).

CHAPTER 2

LITERATURE REVIEW

This chapter describes previous remote sensing and ecosystem studies of mountain ecosystems and alpine vegetation at sites in western North America. These studies provide an insight into the digital image processing techniques employed in previous research for mapping and accuracy assessment in alpine regions. The studies noted here are those that used digitized aerial photography, satellite data, and topographic and digital elevation data. This chapter is divided into three sections of discussion: (a) studies that investigated the biophysical factors and processes influencing the pattern and composition of mid-latitude alpine tundra, (b) remote sensing investigations that include digitized aerial and multispectral data, and (c) investigations the classification and the methods of assessing the classification accuracies used in this research.

Previous High Mountain Ecosystems Investigations

One of the most thorough descriptions of alpine vegetation in the Rocky Mountains of North America was written by Billings (1988). He described the alpine biome as one of the smallest (in area) of the major North American ecosystem complexes. The alpine occupies high mountain summits, slopes, and ridges above the upper limits of forests. In response to intense radiation, wind, cold, snow, and ice, most alpine vegetation is characterized as short, low growing, dwarf shrubs, trees, and perennial herbaceous plants less than a few centimeters tall. Vegetation types vary from “lawn-like” meadows in moist or wet sites, to dry “fellfields” on windward slopes, to

battered cushion plants and lichens on rocky ridges, and to barren areas with persistent or long-lasting snowdrifts, screes, and/or rock cliffs (Billings 1988).

Billings (1988) observed that wind is a strong modifying factor in alpine environments. Strong winds blowing snow off peaks and ridges result in a characteristic meso-topographic moisture gradient in alpine regions in the Rocky Mountains. The pattern of alpine vegetation is largely determined by the moisture gradient, ranging from dry, rocky fellfields on windward slopes, to wet meadows and snowbed communities on leeward slopes, and to bogs on valley floors downslope of leeward snowdrifts. This vegetation/moisture gradient results from the complex combination of snow-pack, time of snowmelt, wind speed and direction, slope steepness, and diversity of the extent flora. The prevailing wind direction in the mountains of the middle latitudes is from the southwest and results in west and southwest windward slopes being snow-free or with relatively shallow snow-pack. Eastern and northeastern slopes accumulate the deep drifts that provide moisture for alpine vegetation on leeward slopes and valley bottoms. Available soil moisture along this topographic moisture gradient is a primary controlling factor for the composition, productivity, and distribution of alpine vegetation species.

Table 2 summarizes alpine plant communities identified by Billings (1988) that occur along transects of the topographic moisture gradient observed during field surveys and studies from several sites in the central and northern Rocky Mountains of Colorado, Wyoming, and Montana.

Table 2

Alpine Tundra Plant Communities

Prevailing Wind Relationship	Community	Topographic Position
1. Windward Slope	Open, Rocky Fellfield	150 m below ridge top to ridge top
2. Upper Lee Slope	Modified Fellfield	Ridge top to 40 m below ridge top
	Early Snowbed	40 – 60 m below ridge top
3. Middle Lee Slope	Early Snowbed	60 – 90 m below ridge top
	Late Snowbed	90 – 120 m below ridge top
	Moist Meadow	120 – 150 m below ridge top
4. Lower Lee Slope	Late Snowbed	150 – 160 m below ridge top
5. Bottom Lee Slope	Wet Meadow and Bog	260 – 300 m below ridge top

Mountain Environments

Billings (1988) found that since mountaintops vary in elevation and latitude, their environments differ in spite of sharing many environmental characteristics in common. These differences are more easily seen along various environmental gradients. The most obvious of these gradients are latitudinal (from equatorial to polar regions) and elevation (from lower slopes to the summits). Billings (1988) noted that these “macrogradients” have a great deal of influence on the amount solar radiation received, the length of day, temperatures, and amounts of precipitation. As one result, such gradients have considerable control of the kinds of plants and animals which are available in the region

to make up the biological parts of mountain ecosystems (Billings 1988). Within the large gradients are smaller environmental gradients which exist on every mountain. These, along with bedrock differences, control almost all the local distribution patterns of plant and animal species within the constraints set by the elevation gradient on that particular mountain.

The smaller gradients are determined primarily by topography. Topography, in itself, does not control growth and distribution of the alpine organisms but does moderate those factors which interact directly with the organisms: solar radiation, soil moisture, soil and air temperatures, wind, and both the blasting and protecting aspects of snow. Ridges, slopes, valley and cirque floors act together along what Billings (1988) called a “mesotopographic” gradient.

A mesotopographic gradient crosses a ridge top and descends the lee slope to a small valley or to a cirque floor in a distance of 50 to a few hundred meters or so. Ridge tops are exposed to strong winds and are relatively cold and dry. Snow is blown into drifts on the upper part of the lee slope. Such drifts do not begin melting until the following summer; some do not disappear except in very dry years, if then. Meltwater from the drifts keeps the lower lee slopes moist; this water eventually accumulates in small bogs, tarns and brooks. A mesotopographic gradient strongly modifies the energy-determined latitudinal and elevation gradients by shifting the snow patterns and ultimately, the amount and timing of water available for plant growth. The result is a steep vegetation gradient in which analogs of vegetation along with the whole latitudinal gradient occur in close proximity.

Within mesotopographic gradients, boulders or rock outcrops produce small, elongated snowdrifts in their lee. Small depressions also catch blowing snow. Even these small drifts produce small environmental gradients and the captured snow, because of the winter protection it affords, is reflected in vegetation patches consisting of species needing such protection. Any variation of this nature can result in microtopographic gradient.

Both mesotopographic and microtopographic gradients result in rather orderly patterns in high mountain environments. These environmental patterns result in vegetation and biological community patterns that match the environmental patterns. Billings (1988) found it convenient to utilize a series of mesotopographic units on a single mountain when studying high mountain ecosystems. The combination of a mesotopographic unit with its microtopographic units and variations in bedrock produces certain patchiness in high mountain environments. Because of the gradients, there is some orderliness to this patchiness.

Billings (1988) also noted that it is the physical factors which dominate and control the ecosystem. The plants and animals are there in patterns determined by local gradients in solar ultraviolet and visible radiation, net radiation, low soil and air temperatures, snow distribution, wind speeds, length of "growing" or snow-free season, steepness of slope, type of rock, and soil characteristics including soil frost action. Plants (alpine vegetation) are small in these cold, windy environments. Vegetation cannot modify or "soften" the environment, as does a montane forest lower down the slope. Consequently, the biological portion of the environment seems to be less important than

physical factors in determining patterns and growth rates in alpine biological communities.

Synthetic Alpine Slope

Burns and Tonkin (1982) developed a Synthetic Alpine Slope (SAS) model as a spatial soil-geomorphic threshold model for alpine environment. The model is based on the spatial relationships between aspect, topography, seasonal snow accumulation, and the distribution of plant communities and alpine soils. The direct relationship between alpine vegetation and their study area were confirmed by their field observations (e.g., soil pits). They concluded that variations in soil characteristics follow topographically controlled variations in snow cover and that the distribution of snow cover controls the distribution of soils. A dimensionless measure of topography, the SAS is similar to the previously mentioned mesotopographic unit of Billings (1988). It is different in that SAS contains more specific components. Each of the seven microenvironment sites of the SAS is defined by an edaphic-topographic snow cover relationship as shown in Figure 3. The extremely windblown (EWB) sites are found on the tops of the drainage divides on the ridge crests and knolls. Extremely windblown, these sites are dry with sparse vegetation, primarily cushion plants. The wind blown (WB) sites are located from the tops to 30% down the drainage divide. Mixed vegetation of cushion plants, sedges, and herbs, are also very dry. Minimal snow cover (MSC) sites occur in similar positions on the drainage divides as the WB sites and generally have more snow cover in the winter months than the WB sites and usually contain thick turf vegetation, primarily kobresia.

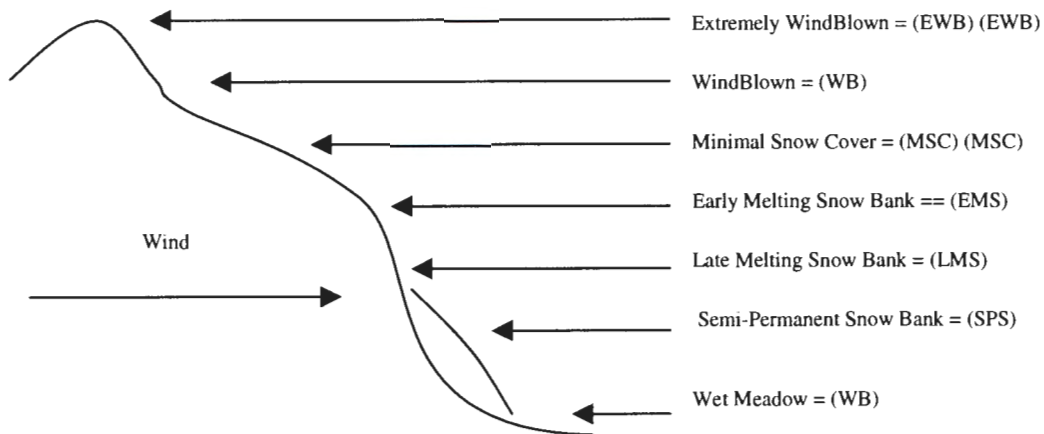


Figure 3. Synthetic Alpine Slope Model: Microenvironmental sites on the leeward side of the slope as described by Burns (1980) and Burns and Tonkin (1982).

Early melting snowbank (EMS) sites are located 30% to 90% of the way down on gentle slopes with a greater variety of vegetation. Snowbanks persist in this location during the winter months but usually melt completely by early June. Late melting snowbank (LMS) sites are present 50% to 90% of the way down the drainage divides in leeward nivation hollows. In these sites, snowbanks melt out in early July and August. The sites are characterized as quite rocky with sparse vegetation. Semi-permanent snowbank (SPS) sites, which are found 60% to 90% of the way down the drainage divides in nivation hollow. Snowbanks rarely melt and generally contain no vegetation and have usually undergone downslope movement producing lobes and terraces. Wet meadow (WM) sites are characterized by bog vegetation and are situated below snowbank sites in depressions and on turf-banked terraces and lobes at the bottoms of

drainage divides. Meltwater from winter snowbanks and snowbanks farther upslope generally cover these sites contributing to the WM saturated conditions.

The SAS model shown in Figure 3 is for leeward slopes but similar slope models occur on windward slopes as well. The windward slope is characterized by generally having less snow accumulation. LMS and SPS sites do not usually occur there while WB and MSC sites extend further downslope.

Alpine Vegetation Classes

In spite of the variety of plant life forms, most alpine vegetation is dominated by perennial graminoids (grasses). Almost all perennial graminoids have much more living tissue below ground than above. Annual species are absent or very few in number. Annual plants are miniature and contribute little to vegetational cover or productivity. Associated with these grasses and sedges are herbaceous dicotyledons and dwarf shrubs. The most productive and luxuriant alpine vegetation lies in the meltwater meadows below melting snowdrifts. The least productive and most sparse vegetation lies under the snowdrift itself and is exposed only in late summer. Here, a few dwarf perennial dicotyledons are the only plants scattered over barren rocks, gravel, and a bit of soil. Table 3 lists a scheme proposed by Billings (1988) for classifying Rocky Mountain alpine plants.

Alpine plants of the middle latitudes are dormant for 9 to 10 months of the year. During this time, temperatures of the surrounding air and soil are at or below freezing. The plants are snow covered except on the wind-swept ridges where snow cover is sporadic. A number of kinds of plants on these ridges or upper windward slopes actually

cannot tolerate protective snow cover and occur only where high winds of winter keep the ground bare and frozen. Among these are sedge (*Kobresia*) and certain small rosette

Table 3

Classification Scheme of Alpine Plant-Growth Forms

Alpine Plant	Growth Form
1. Perennial Herbs	Ferns Dicots Graminoids Lycopodioids
2. Perennial Cushion Plants	
3. Giant Rosette Plants	
4. Shrubs (Dwarf or Prostrate)	Deciduous Evergreen
5. Succulents	Stem (Cacti) Leaf (Sedum)
6. Annual herbs	Dicots Gramminoids
7. Lichens	
8. Mosses	

saxifrages and cushion plants. Such plants, in dormant condition, are adapted to environmental conditions which seem as severe as any on earth: extremely cold and dry because of exposure. The perennating or live parts of alpine plants in long-winter

mountains are in the buds, roots, and rhizomes; in evergreen plants, the younger leaves also remain alive.

Remote Sensing Investigations

During the past two decades, great strides have been made in the applications of computer technology to assist in the interpretation of multi-spectral data (Jensen, 1996). Most of the research involving digital processing of multi-spectral data for the identification of land cover has been applied to electro-optical scanning systems (Landsat or airborne scanners). Some authors have investigated the use of computer assisted interpretation of digitized aerial imagery and have documented the benefits and problems associated with this technique (Jensen & Estes, 1978; Mace & Bonnicksen, 1982; Quirk & Scarpace, 1982; Scarpace, 1978; Scarpace, Quirk, Kiefer, & Wynn, 1981; Tucker, 1979; Turner & Thompson, 1982). One of the crucial components in the analysis technique is the knowledge of the relationship between light striking the film and the resultant film density (Scarpace, 1978). Many investigators have reported techniques to determine this relationship. Largely oriented toward quality control of film processing, these techniques are also applicable to analysis of remote sensing imagery. Some investigators have applied calibration techniques to photographic imagery exposed for remote sensing purposes (Scarpace, 1978).

Aerial Photography and Multispectral Investigations

Manual interpretation of aerial photographs have been widely used to inventory land cover. However, this can be a labor-intensive process with inconsistencies among photo interpreters. Digital interpretation has several advantages over manual

interpretation. It permits mathematical transformations and enhancements of the imagery (Jensen & Estes, 1978). It can also reduce bias and inconsistency among interpreters due to differences in skill levels, fatigue, and other factors. However, human interactions with digital analysis is still required. By digitizing the photographs, the advantage of computer aided interpretation can be combined with the fine resolution of aerial photography (Jensen, 1996).

As a result, there has been an increase in the use of remote-sensing techniques used by scientists and federal agencies that provide an economical means for obtaining vegetation mapping data. In particular, the analysis of black and white, color, and color infrared photographs, to inventory and monitor alpine regions (Becking, 1959). Aerial photography provides rapid collection of large amount of data as well as providing a true overview of an area. The interpretation of large-scale imagery (1:10,000 to 1:40,000) has been an integral part of many land-related studies. For example, mapping land-cover and land-use classification, forest management, geology, and geography (Jensen & Estes, 1978).

Becking (1959) evaluated black and white aerial photography for mapping small tundra communities, but concluded that, even though small mapping units could be recognized on large-scale photography, vegetation type could not be interpreted. Vegetation cover, or density, was the primary control over tonal variation on the photography, which is not necessarily associated with vegetation types. Keammerer (1976) mapped broad vegetation types in the Colorado Rocky Mountain Front Range with color infrared aerial photography. She was not able to distinguish vegetation type

directly on the imagery, but she could classify landscape characteristics associated with vegetation distributions directly from the imagery.

Frank and Thorn (1985), Frank and Isard (1986), and Frank (1988) developed remote sensing techniques to map alpine tundra in the Colorado Rocky Mountain Front Range. They used digitized aerial photography, developed topoclimatic indices, and processed Landsat Thematic Mapper (TM) digital imagery to map the alpine vegetation classes found in Table 4.

Table 4

Alpine Vegetation Classes

Alpine Vegetation
1. Wet Herbaceous Meadow (Sedge-Elephantella)
2. Dry Herbaceous Meadow (Golden Banner – Yarrow)
3. Moist Alpine Meadow (Apline Avens Alpine Meadow)
4. Dry Alpine Meadow (Kobresia)
5. Dry Alpine Meadow (Sedge-Kobresia)
6. Rocky Alpine Meadow (Moss Campion Fellfield)

Frank (1988) compared his classification results with a large-scale vegetation map prepared using field surveys manual cartographic techniques. He reported the following results: (a) Classification accuracy's for herbaceous meadows, 84.44 %; moist alpine meadows, 66.31 %; and dry alpine meadows, 86.73 %; (b) fellfield communities were not

distinguishable from dry alpine meadows because spectral and topoclimatic difference were not sufficiently different at the resolution of the database; and (c) wet alpine meadows were not distinguished from wet herbaceous meadows because the spectral characteristics were similar even though elevation difference existed between the two communities. Alpine meadow were identified more accurately than Frank (1988) expected considering the spatial resolution of Landsat TM and the DEM. He suggested the models used in this study would be useful for mapping other alpine communities in the Rocky Mountains.

Frank and Thorn (1985) found that alpine tundra distributions could be mapped using a two-stage classification system that combined digitized aerial photography with digital elevation, slope, and aspect data; however, the method was difficult to extend beyond the local study sites. Frank and Isard (1986) developed a more generalized method to combine digitized aerial photography with topoclimatic indexes to map alpine tundra, but the topoclimatic indexes were not readily transferable to surrounding areas. Cybula and Nyquist (1987) used a similar method to characterize vegetation distributions by combining Landsat MSS, topographic, and general participation inferred from watershed delineation's. Smith and Pittman (1996) used digital imaging processing techniques of scanned NAPP photography to successfully map forest species delineation in the area of Fort Jackson, South Carolina.

Frank (1988) combined Landsat TM data with topographic and topoclimatic variables to map dominant vegetation communities in the Colorado Rocky Front Range. The best Landsat TM transformations used as predictor variables were found by

calculating a discriminant function for each observation, then calculating the correlation between each predictor variable and the discriminant function.

Digitized photographs have been used with varying degrees of success. Accuracy depends on the detail of the information desired and the use of proper correction procedures. Hoffer, Anuta, and Phillips (1972) reported accuracies of 94% and 95% for digitized 1:120,000-scale color infrared (CIR) and black and white multi-band imagery, respectively. Quirk and Scarpace (1982), working with digitized 1:24,000-scale CIR photography from the Green Bay Wisconsin area, concluded that the analysis of a digitized photograph could analyze large areas at a finer resolution than manual interpretation.

Mace and Bonnickson (1982) compared digitized 1:120,000-scale CIR photography with Landsat multi-spectral scanner (MSS) data for classifying forest-cover types on the Apostle Islands in Wisconsin. Some film calibration techniques were followed except that the vignetting correction was omitted because the small study area was close to the area of the principal point. Ground resolution was set at 36 meters. Overall, classification accuracies for the MSS were less than for the digital CIR data (47.9% and 68.3%, respectively). Results concluded that accuracies increase as the detail of land-cover classes are decreased by aggregating forest type classes.

Turner and Thompson (1982) digitized eleven 1:21,000-scale CIR photographs to classify a North Carolina barrier island into water, sand dune, mesic shrub, xeric shrub, shrub thicket, pine woodland, and high and low salt marsh. In this case, no film calibration was applied to the digital data. The overall classification accuracy was 62%.

The classification accuracy for vegetation was 48%. The authors noted that both film calibration and a classification technique more suited for remote sensing might have increased accuracy.

Jensen and Estes (1978) indicated that vignetting can severely reduce the accuracy for digital analysis of multi-temporal high altitude CIR photographs. Efforts were made to reduce the effects of vignetting by using anti-vignetting filters on the camera system and preprocessing the digitized density values by an anti-vignetting algorithm. However, signature extensions of crop types across the digitized photography was still hampered by vignetting effects.

Classification and Accuracy Assessment Investigations

Assessing the accuracy of classification of remotely sensed data is a necessity. Traditionally the accuracy of photointerpretation has been assumed 100% correct. However this assumption is rarely valid. Due to the complexity of digital classification, the necessity for accuracy assessments of the results is greater (Congalton, 1991). In the mentioned research, the only study that reported an accuracy assessment was the photointerpretation of Landsat MSS by Knepper (1977). The other studies used automated classification routines to classify the digital data but did not report on the accuracy of the resulting classification. In this research, the field data are gathered and used in rigorous statistical accuracy assessment.

The classification techniques used in the studies reviewed included both supervised, unsupervised methods, and as linear discriminant analysis. Linear discriminant analysis has often been used to classify remotely sensed including recent

studies in mountainous terrain using a DEM (Franklin & Moulton, 1990; Franklin & Wilson, 1991). The linear discriminant classifier is preferred for hypothesis testing with the maximum likelihood classifier because it is more robust and handles the assumptions of mild violations are better tolerated (Huberty, 1994). The output from the discriminant analysis is tabular with no map output. The combination of the two classifiers (linear discriminant functions and maximum likelihood) can be accommodated in a methodology as demonstrated by Franklin and Moulton (1990). The discriminant analysis can be used for the classification with attribute tables for output and the maximum likelihood classification can be used to show the spatial distribution of the results with a map output. This research is based on this methodology which was developed by Franklin and Moulton (1990) for general landcover classifications.

The study by Walsh (1987) used a DEM in the analysis but not in the classification stage. Instead, the DEM was applied after classification in a GIS environment. DEMs should be included in the analysis of spectral response patterns of mountainous regions (Walsh, 1987) to reduce partially the topographic effect (Holben & Justice, 1981). Studies have proven that topography represented by a DEM is an independent source of information that improved classification accuracies for both Landsat MSS (Franklin & Ledrew, 1983) and TM data (Franklin & Moulton, 1990). A DEM Treated as ancillary data can be incorporated into a classification routine in a number of different ways including: (a) preclassification scene stratification, (b) postclassification sorting and (c) logical channel classification (Hutchinson, 1982). Recent developments for incorporating ancillary data into classifications are a three stage

classifier by Franklin and Wilson (1992) and evidential classification (Franklin, Peddle, Wilson, & Blodgett, 1991). As mentioned, this research used the basic logical channel method where the DEM variables will be included in the classification as normal input channels with the digitized NAPP data because the technique has proven successful when the objectives include assessment of classification accuracy with and without ancillary data (Franklin, 1987).

The number of vegetation types that can be classified using remote sensing imagery is large and not yet fully known (Frank & Thorn, 1994). One of the remaining goals of remote sensing in mountain environments is to find a means for extending local scale observations and models to larger, geographic regions.

CHAPTER 3

METHODOLOGY

This chapter describes the data and the methodology for this research. The first section describes the acquisition and processing of the four main data sets: (a) Global Positioning System data collection (b) field data (c) the digitized NAPP image and (d) the DEM data. The second section provides an overview of the methodology used for digitizing the NAPP imagery. The third section summarizes the classification methodology used to integrate the digitized NAPP Imagery and the DEM. The methods were previously developed by Franklin and Moulton, (1990), Franklin and Wilson, (1992) and were published in a series of papers by Hutchinson (1982), Franklin and Ledrew (1984), Walsh (1987), Franklin and Moulton (1990), and Franklin and Wilson (1992).

Four sets of data were required for this research: (a) Global Positioning System data, (b) documented vegetation data of the study area, (c) digitized NAPP data, and (d) DEM data. The Global Positioning System data provided the three-dimensional location information for each site, the vegetation data includes field data at each site, which consists of topographic data and percentage surface cover. The digitized NAPP data includes reflectance values for each spectral band and topographic data was extracted from a DEM for each pixel in the study area. These data sets are used to determine if the unique spectral and geomorphic signatures of the alpine vegetation can be captured and used to train a classifier for a supervised classification.

Global Positioning System Data Collection

GPS data were collected at each location during field surveys conducted in August 1998. The Trimble Navigation Geoplotter II, a six channel, Coarse/Acquisition (C/A) receiver, was used to collect GPS data for each ground control point (GCP) and vegetation region used in this study.

GPS site survey data included GCP of selected monuments and landscape features, vegetation sample locations and elevation profiles. Landscape features consisted of rock formations at separate peaks of the study area and well-defined lake boundaries and trail intersections.

The GPS base station data used here were recorded and archived by University of Wyoming and the Bureau of Land Management (BLM) personnel at the BLM Casper District Office in Casper, Wyoming, for August 8th and 9th, 1998. Base station files consist of GPS horizontal and vertical positional data collected at the base station (a known point) for a 24-hour period corresponding to each day of the alpine vegetation site surveys. The base station data were required for post-survey differential corrections of the GCP and site survey data to correct the systematic error (i.e., Selective Availability) induced in the GPS signal by the Department of Defense. By determining the difference between the known position of the base station and position computed from the data recorded for a specific 24-hour time period, a correction factor can be determined and applied to remote GPS survey receivers within 300 miles of the base station to remove most of the systematic positional error induced by Selective Availability.

The position of the BLM Casper Community Base Station antenna (Table 5) was determined by static differential GPS survey to a relative three dimensional accuracy of 5 cm with respect to the Wyoming High Accuracy GPS Network (HARN). The GCP's and GPS site survey data collected during August 1998 are presented in Table's 6, 7, and 8.

Table 5

Casper GPS Community Base Station (CBS)

Base Station Parameters	
Latitude:	42° 51' 23.43144" North
Longitude:	106° 18' 11.02347" West
Antenna Height Above Ellipsoid (HAE):	1554.313 Meters
Datum:	NAD 1983/1993
Ellipsoid:	GRS 1980

Field Data

Field data collection involved the identification of biophysical variables that were thought to affect location, composition, and pattern of alpine tundra on Roaring Fork Mountain. The variables included (a) topoclimatic variables (e.g., horizontal and vertical location, slope, aspect, slope configuration, topographic position) (b) biogeographic variables (plant communities), and (c) geomorphic variables (e.g., landforms, structures, geomorphic processes). The variables were observed and/or measured through a

Table 6

Roaring Fork Mountain Global Positioning System Data Collection August 8, 1998

Rover Files	Casper CBS Files	DGPS Corrected Files
R080809a.ssf R080809b.ssf R080809c.ssf	C8080809.ssf	R080809a.cor R080809b.cor R080809c.cor
R080810a.ssf R080810b.ssf	C8080810.ssf	R080810a.cor R080810b.cor
R080811a.ssf R080811b.ssf R080811c.ssf R080811d.ssf	C8080811.ssf	R080811a.cor R080811b.cor R080811c.cor R080811d.cor
R080812a.ssf R080812b.ssf	C8080812.ssf	R080812a.cor R080812b.cor

Table 7

Roaring Fork Mountain Global Positioning System Data Collection August 9, 1998

Rover Files	Casper CBS Files	DGPS Corrected Files
R080908a.ssf	C8080908.ssf	R080809a.cor
R080909a.ssf	C8080909.ssf	R080909a.cor
R080910a.ssf	C8080910.ssf	R080910a.cor
R080913a.ssf R080913b.ssf R080913c.ssf	C8080913.ssf	R080913a.cor R080913b.cor R080913c.cor
R080914a.ssf	C8080914.ssf	R080914a.cor

Table 8

Roaring Fork Mountain Ground Control Point Global Positioning System Data CollectionAugust 9, 1998

GCP Files	Casper CBS Files	Phase Processed DGPS Corrected Files
R080910b.ssf	C8080910.ssf	C8080910.cor
R080914c.ssf	C8080914.ssf	C8080914.cor
R080921a.ssf	C8080921.ssf	C8080921.cor

combination of field reconnaissance and remote sensing techniques. A stratified random sampling method of the study area was used for site selection.

Vegetation and topographic data for the study area were previously collected by Dr. Richard W. Scott (1970). Scott's survey was conducted during the first two weeks of August 1970. It provides a temporal match in the growth cycle of the alpine vegetation as compared to the anniversary date of the NAPP photography (7-31-89) and the GPS field survey of August 8-10, 1998. Ground data were gathered to describe the morphology and surface cover of the sample of each site. The basic morphology of a site can be described with the topographic variables of elevation, slope, and aspect as outlined in the general system of geomorphometry (Evans, 1972). Scott originally measured these variables as feet above sea level, degree of slope, and degree of azimuth, respectively as described in Table 9. Figure 4 illustrates the vegetation sites chosen Scott used in this study. The number of samples is an important consideration when designing the sampling scheme. For study areas with less than 12 land-cover classes, a minimum of 50 random

Table 9

Richard Scott's Topographic Data for Alpine Vegetation Located on Roaring Fork Mountain, Wyoming

Plot	Elevation	Aspect	Slope	Description
708	10,600	228°	30°	Just above timberline. Soil is very thin, stony, coarse fragments
709	10,700	246°	22°	Aprox. 80ft higher then 708. Soil is stony but more stable than that of 708
7010	10,700	252°	19°	100ft North and 20 ft upslope from 709. Veg, dense, taller
7011	10,800	224°	26°	Rocky, wind swept ridges. Soil is very thin, stony, ozonal, coarse, fragments
7012	11,100	252°	12°	Small alpine slope surrounded by fellfield boulders
7014	10,600	239°	14°	Lush meadow above water seap
7015 -7020	10,950	216°	0°	Very wet, Wet seap.
7021 -7025	10,950	216°	15°	Up from 7020 along the bank
7026	10,840	280°	11°	Salix Planifolia thickets along small stream
7027	11,100	273°	9°	Salix Planifolia thickets along small stream

(table continues)

Plot	Elevation	Aspect	Slope	Description
7028	11,100	300°	0°	Dryer than 7027
7029	11,360	330°	8°	Moist Geum turf located approx. 6ft from meltwater stream
7030	11,400	0°	0°	Wind Swept saddle on Roaring Fk. Mt. Coarse material
7031	10,950	0°	0°	Wind swept ridge. Very little soil, coarse rocky material.
7032	11,100	61°	9°	Exposed rocky ridge w/ large boulders
7033	11,120	0°	5°	Wind Swept saddle between Stough CK and Leg Lake
7034	11,100	237°	6°	Sheetwash slope, poorly vegetated. Small particles of qtz and feldspar
7035	11,300	2°	18°	Late snowmelt area Bare ground
7036	11,450	325°	7°	Summit of one of Roaring Forks peaks with many large, wind eroded rocks w/ veg. in between
7037	11,300	308°	12°	Turf
7057	11,100	60°	1°	Meltwater streams, freeze/thaw activity

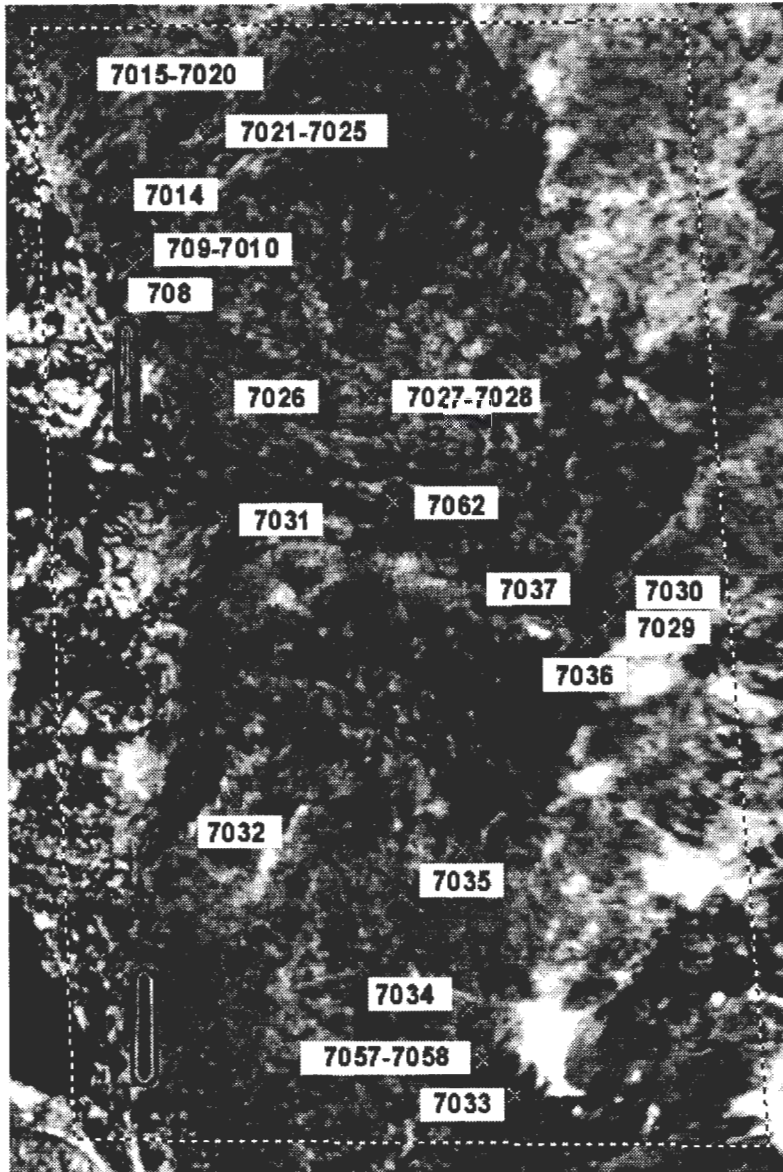


Figure 4. Vegetation sites selected by Scott and subsequently revisited and geolocated using GPS. Scale 1:18000.

samples per class is recommended (Congalton, 1991). However, the number of training samples can be adjusted based on the importance of each class. Sampling can be increased in important classes and decreased in less important classes. In this study, the number of samples varies from 6 to 81 per class, for a total of 256 samples or pixels (Table 10).

Table 10

Classification System and Number of Training Samples/Pixels

Class	Class Name	Number of Samples/Pixels
1.	Moderately Drained Tundra Meadow	69
2.	Dry Meadow	6
3.	Exposed Fellfield/Moist Vegetation	81
4.	Exposed Fellfield	39
5.	Moist Tundra Meadow	61
Total		256

Integrating the NAPP Imagery

The NAPP aerial photograph of the Roaring Fork mountain study area was originally acquired on July, 31 1989 with a sun elevation of 49.3°, azimuth of 138.1°, on flight path 8313 and flight row 1182, using Kodak Aerochrome 2443 color-infrared (CIR) film. NAPP photographic coverage is designed for a wide variety of applications

in that its black and white photographs are panchromatic (wavelength, 0.47 - 0.73 μm) and its CIR images are a multispectral film composite. That is, the CIR film simultaneously records in the green (wavelength, 0.5-0.6 μm), red (wavelength, 0.6-0.7 μm), and the near infrared (wavelength, 0.73-0.90 μm) parts of the spectrum as seen in Figure 5 (Kodak Aerial Services, 1996). For a complete explanation of the NAPP program and its parameters please refer to Appendix A.

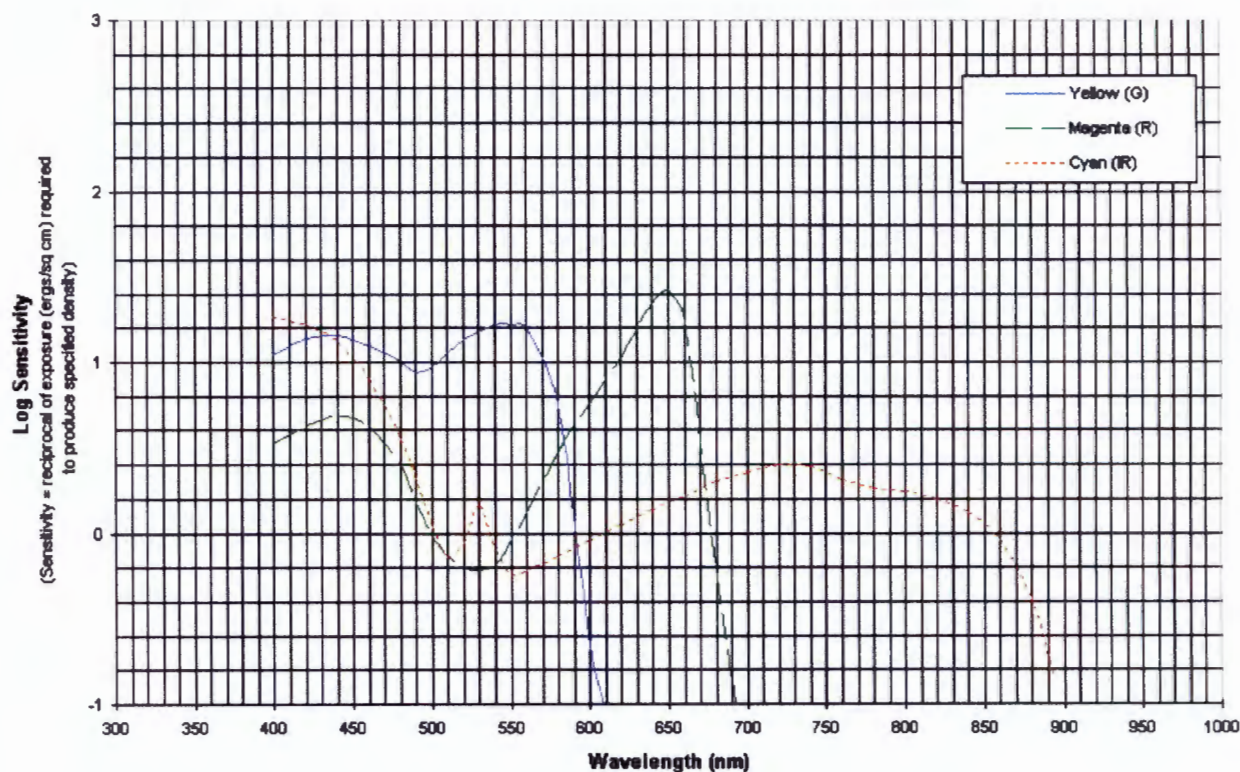


Figure 5. Spectral Sensitivity Color infrared films are sensitive to ultraviolet, visible, and infrared radiation to approximately 900 nm (Kodak Aerial Services, 1996).

Digitizing the NAPP Imagery

Light (1993) summarized the optimum methods for converting the NAPP data into a national database of digitized photography that meets National Mapping Accuracy Standards. Microdensitometer scanning of the photography using a spot size of 25 μm preserves the 27 resolvable line-pair-per-millimeter (lp/mm) spatial resolution in the original NAPP photography. This yields a digital image that has a ground spatial resolution of ≤ 1.0 m, depending on the original scene contrast. This meets most land-cover and land-use mapping user requirements (Light, 1993). The digitized information can be color separated into separate bands of information.

To meet the mapping standards as defined by Light (1993) the computation of pixel ground resolution was accomplished using the parameters defined in Table 11. The analog to digital conversion of the 1:40000 scale NAPP (23cm x 23cm) image was done on a Howtek Scanmaster 4500 11.0" x 11.8" optical drum scanner with a tungsten halogen light source. The scanner uses three matched Triple Photomultipliers (PMT) sensors (red, green, blue) set at 25 microns resulting in a three band, 1,000 dots per inch (dpi) image with 1.016 meter spatial pixel resolution. The Howtek scanner used Trident imaging software to write the digital data to the "lossless" image compression (2:1) file format Tagged Image File Format (TIFF). The integer based file format was chosen over other file formats because the lossless compression retains critical pixel information required for effective computer based remote sensing algorithms and is commonly used among the major image processing software packages such as ERDAS Imagine.

The storage requirement for digital image data is large. Obtaining the optimal pixel size (or scanning density) is a trade-off between capturing maximum image information and the digital storage burden. For example, scanning the 23cm X 23cm NAPP image at 25 microns for red, green, and blue results in a file with 9088 rows and 9070 columns. At 8 bits per pixel using lossless image compression, the three band file occupies about 247 megabytes. Scanning resolution versus digital data volume is illustrated in Figure 6.

Table 11

Computation of Pixel Ground Resolution

Method	Formula	Pixels Size in Meters
Using DPI:	$PM = (S/DPI)/39.37$	$(40000/1000)/39.37 = 1.016 \text{ PM}$
Using Micrometers	$PM = (S \times \mu\text{m}) 0.000001$	$(40000 \times 25.40) 0.000001 = 1.016 \text{ PM}$

Note. The NAPP photo digitized for this study is 1:40000 scale scanned at 1000 DPI or 25.40 $\mu\text{m} = 1.016$ Pixels per meter. DPI = dots per inch; μm = micrometers; S = photo scale; PM = pixel size in meters. Adapted from "Introductory Digital Image Processing: A remote sensing perspective," (2nd ed.), by J. R. Jensen, 1996, p. 20. Copyright 1996 by Prentice-Hall.

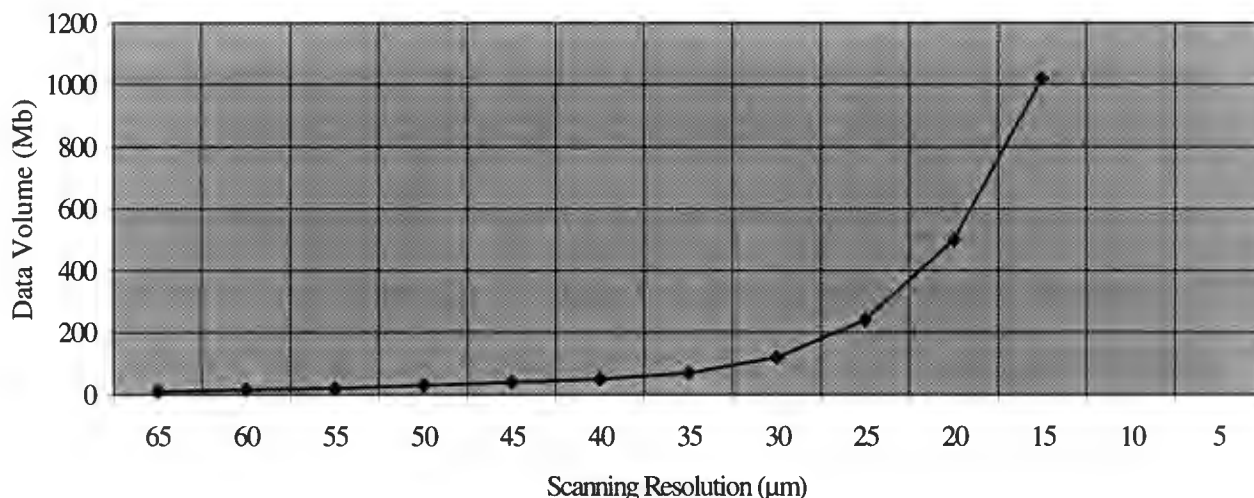


Figure 6. Illustrates data volume increases geometrically as the micrometer is decreased.

For this study, a scanning resolution of 25µm was used to convert the NAPP image.

Image Processing

After data conversion, the histogram for each band of the digitized NAPP imagery was evaluated for its radiometric characteristics and normalized as defined by Smith & Pittman, (1996). Smith and Pittman found that Radiometric Enhancement was necessary with digitized NAPP CIR imagery to separate mineral from vegetation. Radiometric enhancement deals with the individual values of the pixels in the image. Enhancement makes important features of raw, remotely sensed data more interpretable to the human eye (ERDAS, 1994). Enhancement techniques are often used instead or in conjunction with classification techniques for extraction. This is especially critical in alpine vegetation studies to insure information regarding the relationship between vegetation and spectral reflectance can be obtained visually and by computer processing (Franklin &

Ledrew, 1984). Spectral reflectance from green, healthy vegetation is characterized by strong chlorophyll absorption in the red wavelength interval (.63-.69 μm) and reflectance in the near-infrared interval (.76-.90 μm) from plant canopy. Variations from this idealized reflectance model occurs when changes in vegetation vigor and the composition of the surrounding soil background change both spatially and temporally. For alpine vegetation, a decreasing near-infrared /red reflectance ratio is not uncommon in response to slightly increasing vegetation cover (Frank, 1988). This effect occurs when spectral reflectance is modified by the surrounding soil and rock background reflectance. Under this condition, reflectance decreases as vegetation productivity masks the background reflectance.

Histograms of the “raw” digitized NAPP are bi-modal as seen in Figure 7. In order to enhance the spectral differences between alpine vegetation and the surrounding mineral background, the radiometric normalization procedure histogram equalization was applied to the digitized NAPP image. The histogram equalization technique is used because the distinction between dry and moist vegetation, and vegetation and the soil-mineral background were not as pronounced in the digitized image as they were in the original NAPP photograph. Histogram equalization is a non-linear stretch that redistributes pixel values so that there are approximately the same number of pixels with each value within a range. The result approximates a histogram that is more Gaussian in nature and accomplishes two tasks. Contrast is increased at the “peaks” of the histogram and lessened at the “tails” (as seen in Figure 8) enhancing the visual interpretability of the image as well as preparing for the maximum likelihood

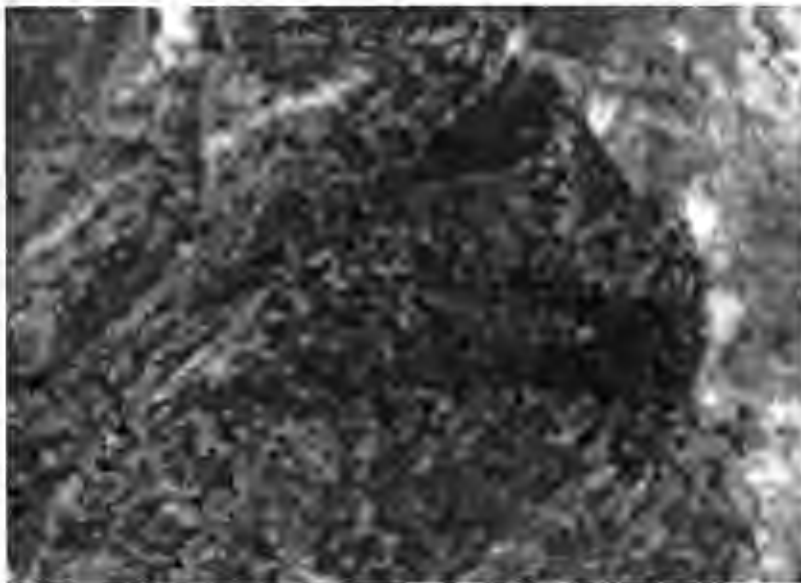
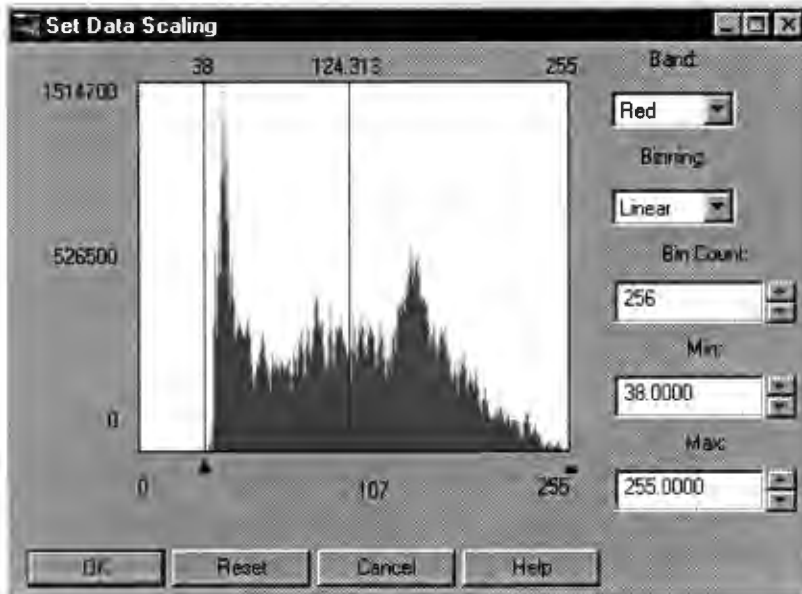


Figure 7. Histogram and image are prior to the application of the histogram equalization.

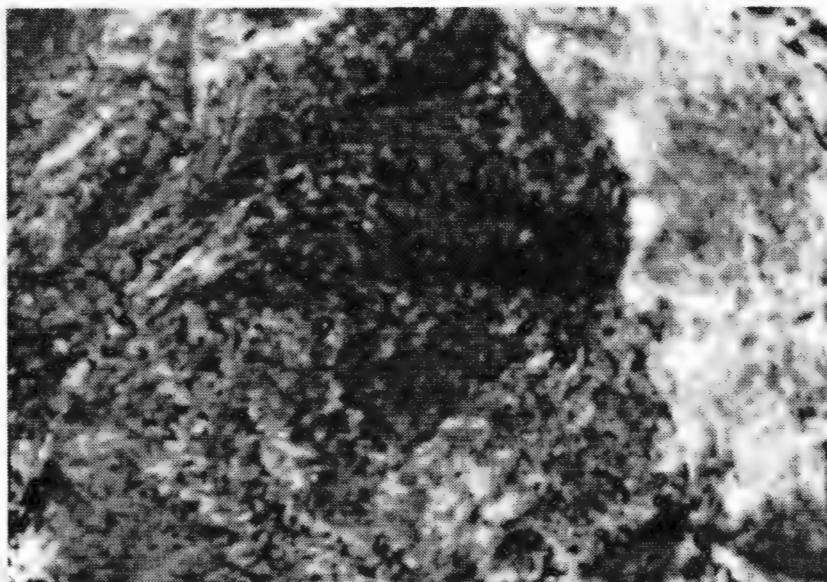
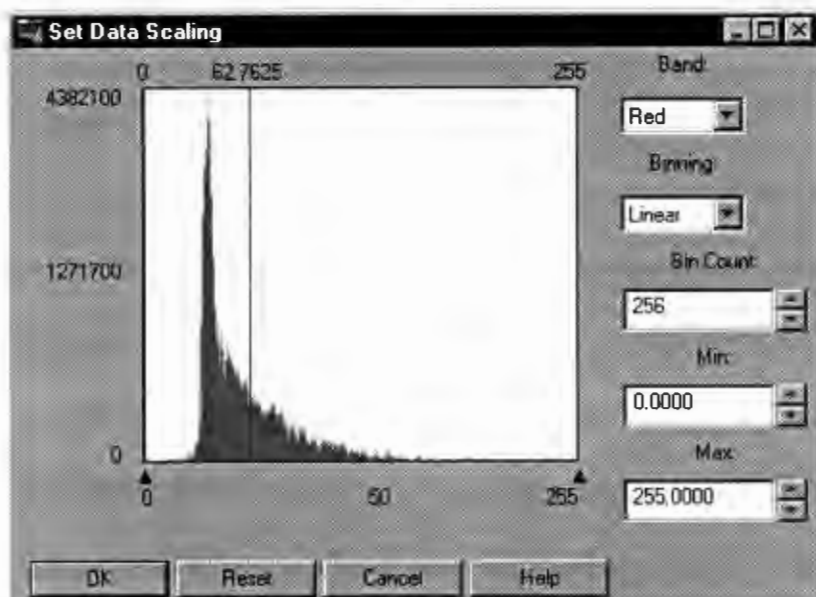


Figure 8. Histogram and image after application of the histogram equalization

classification process which assumes statistics for each band be normally distributed (Erdas, 1994).

Orthorectification

Prior to classification, the digitized NAPP Imagery is orthorectified to the UTM grid system, spheroid Clark 1866, North American Datum (NAD) 27 for zone 12 using the nearest neighbor Orthorectification camera model algorithm in the IMAGINE 8.3.1 (Erdas, 1994). The correction for the image used 12 dispersed ground control points and two mosaiced USGS DEM's resulting in a Root Mean Square Error of 0.476 meters in the X direction and 0.474 meters in the Y direction. Orthorectification model was chosen over the polynomial rectification method because polynomial does not account for elevation which is critical in remote sensing studies in mountainous areas (Figure 9). Before the camera model could be used, the two required USGS DEMs (0f3798 and 0e3799) were mosaiced together. First, they were imported into Erdas Imagine using the DEM import function in the Imagine Import module. The Mosaic algorithm was then used to mosaic the two georeferenced USGS DEM together using the Overlap function, thus, eliminating the need to compensate for the negative numbers commonly dealt with when mosaicing USGS DEMs. The camera lens introduces distortions to the image increasing and radiating from the center of the image outward. Therefore, the scanned NAPP photo is more or less a 3d parabola. The camera model allows you to enter the lens parameters to remove the distortion characteristic of each lens type (provided you have accurate 3d ground control) to create custom geometric corrections for a specific

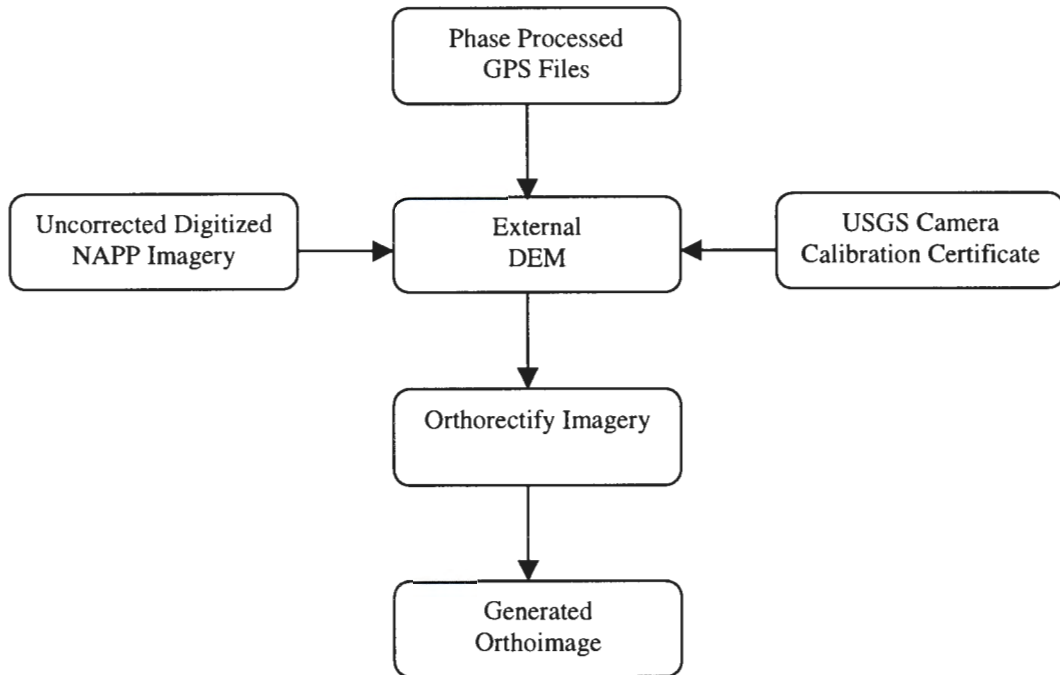


Figure 9. Illustrates the Orthorectification Model used to rectify the digitized NAPP to three dimensions.

camera including principle points, focal length, and fiducials. Figure 10 illustrates the orthorectified color composite scene of the RGB bands 1, 2, 3 of the study area. The digitized NAPP imagery is used as a complete set and as an extracted subset of 256 pixels, which represents the field sites. The field sites were located on the image with the aid of: (a) Scott's vegetation location data, (b) experience of gathering data in the field, (c) the analog copy of the NAPP image, and (d) USGS digital Raster Graphs. These pixels are extracted from the complete set by first creating a pixel coordinate table

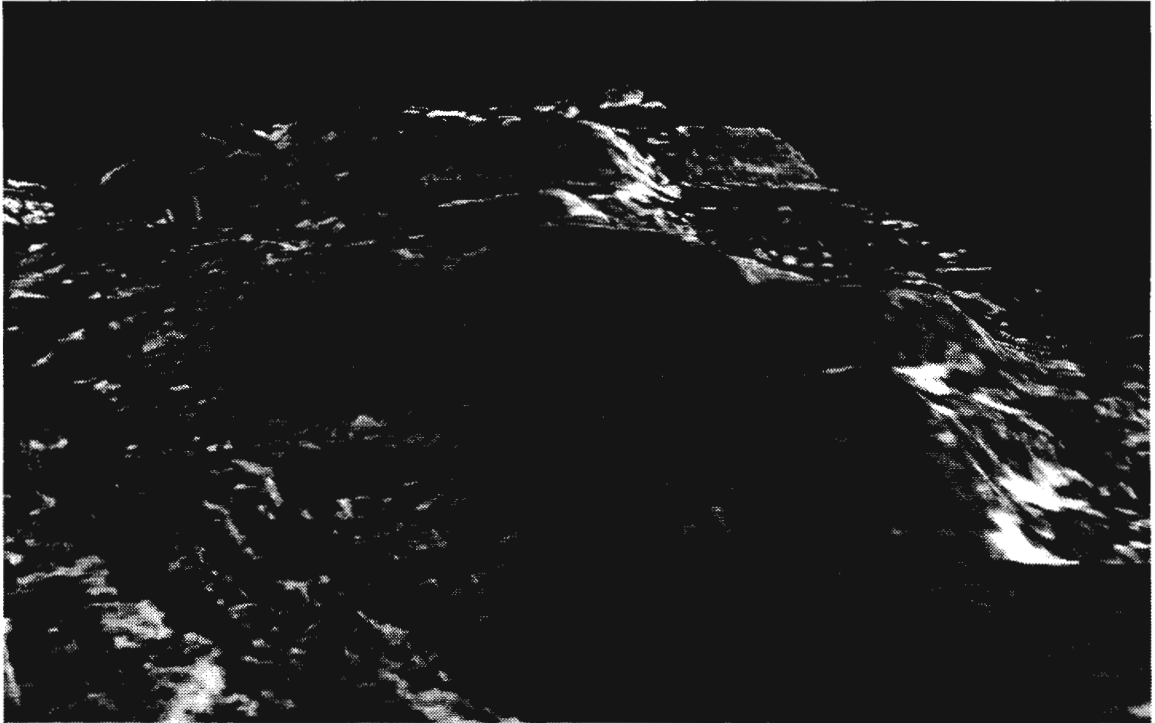


Figure 10. Orthorectified color composite scene of the RGB bands 1, 2, and 3 of the study area. Scale 1:26000.

which contains the class number and X and Y pixel coordinates. This is output to an ASCII format and input to S-Plus for linear discriminate analysis to help determine final classification accuracy. The digitized NAPP dataset is input into the maximum likelihood classifier in ERDAS Imagine to illustrate the spatial distribution of the vegetation classes.

DEM data

Ground measured topographic data are available for 21 sample sites visited in the field. This sample size is sufficient for the linear discriminant analysis (Davis, 1986). To map the entire area for spatial distribution of topographic data, every pixel is required (233,436 in total after subset). The same two USGS DEM's of the study area used in the orthorectification process were acquired on CD-ROM in the Spatial Data Transfer Standard (SDTS) file format. The DEM data for 7.5-minute units correspond to the USGS 1:24,000 scale topographic quadrangle map series for all of the United States and its territories. Each 7.5-minute DEM is based on 30 by 30 meter data spacing with the UTM projection.

Modules are available in ERDAS Imagine to extract slope and aspect from the DEM. The calculation of these topographic variables are discussed in detail by ERDAS Inc. (1994). The slope and incidence values are extracted from elevation, then a window of the DEM that represents the study area, is extracted. Grey level images of elevation are given in Figure 11, slope in Figure 12, and aspect in Figure 13. Aspect (direction of azimuth) is a directional variable that is circular in nature. For example, 10° is closer to 350° than to 50° . This characteristic creates a serious problem with traditional classifiers such as linear discriminant analysis and maximum likelihood classification, which can handle linear data only. To overcome this problem, aspect data must be transformed into a linear scale (Erdas, 1994). The transformation algorithm tested by Hutchinson (1982) and used by Franklin and Moulton (1989) is used in this

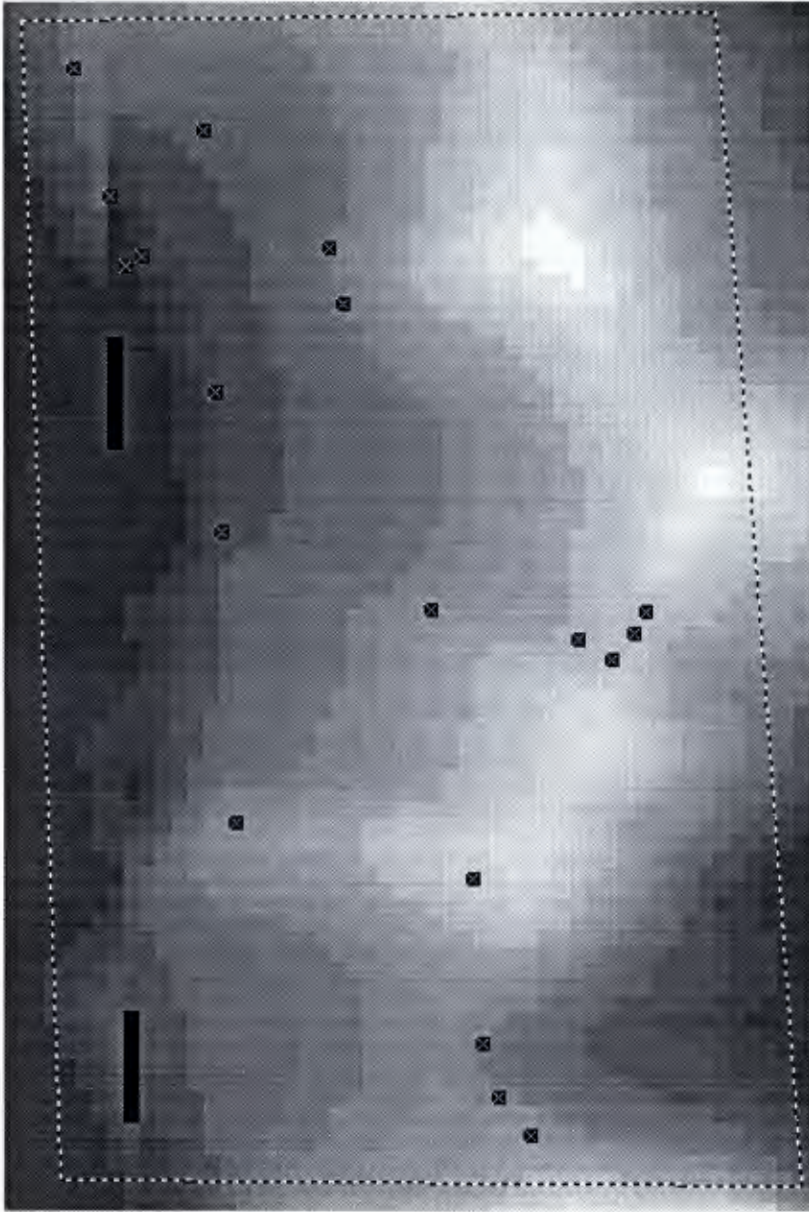


Figure 11. Elevation image of the study area. Scale approximately 1:18000.

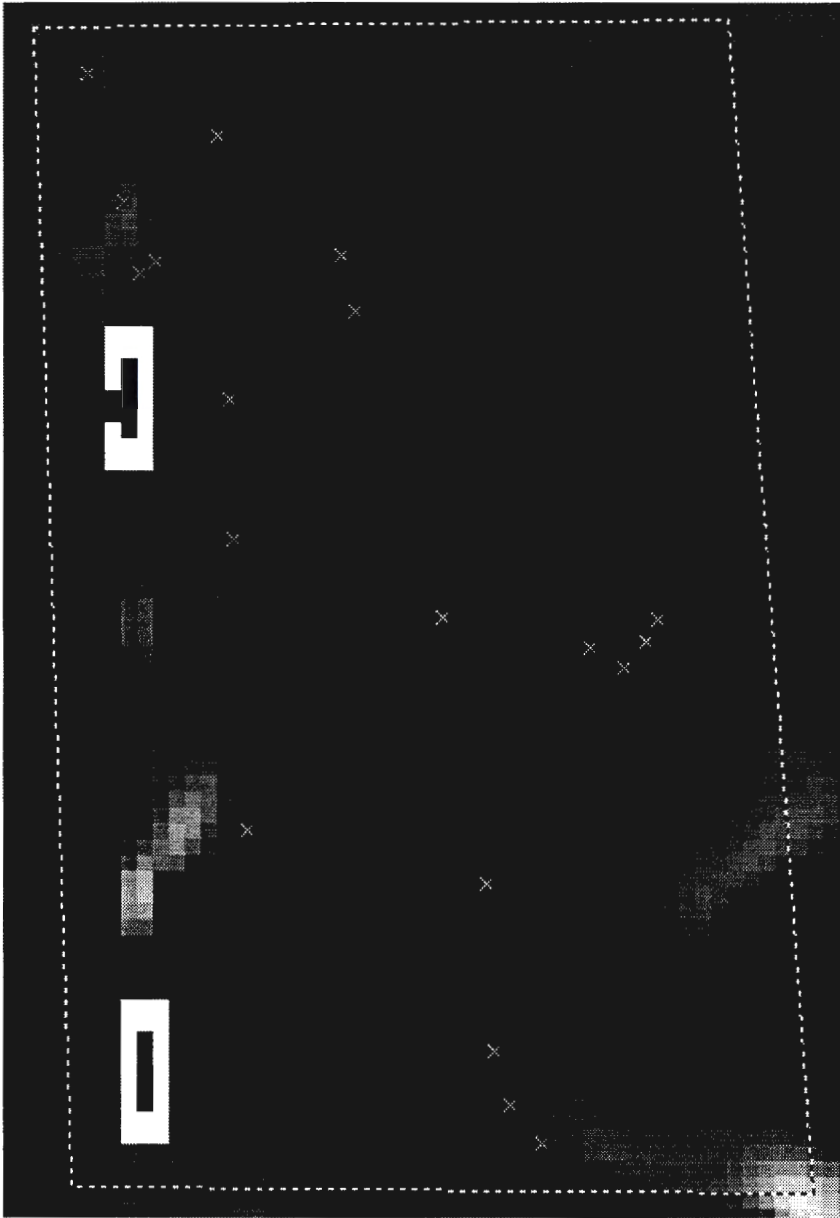


Figure 12. Slope image of the study area. Scale approximately 1:18000.

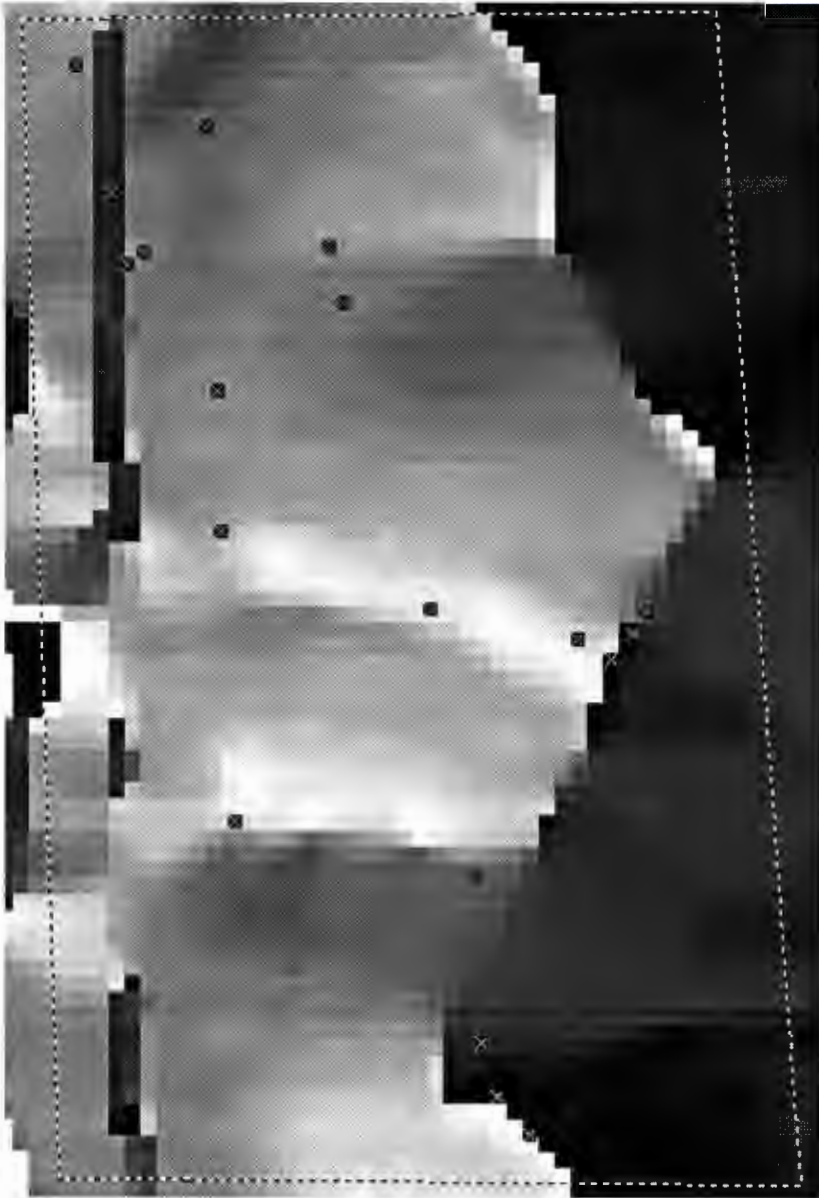


Figure 13. Aspect image of the study area. Scale approximately 1:18000.

study. The algorithm computes an incidence value as a function of site or pixel specific aspect and slope values, and constants of solar elevation and solar azimuth values, of the digitized NAPP image.

The Grey level values of elevation, slope and aspect were extracted from the DEM for the 256 pixel samples and added to the digitized NAPP attribute table. This file was input into the linear discriminant analysis to determine the increased accuracy that can be achieved by the DEM variables alone and the increase in accuracy when added to the digitized NAPP data set. The mosaiced DEM was later evaluated with the digitized NAPP data set for maximum likelihood classification output of landcover map.

Classification of Digitized NAPP Imagery and DEM Data.

As previously mentioned, an unsupervised classification of the imagery can provide insight into the landscape types of a study area, aiding in the selection of sample sites for the stratified sampling method. For this research, the unsupervised classification of the digitized NAPP imagery was performed first and then compared to Scott's existing vegetation. This is accomplished using the widely used clustering algorithm called Iterative Self-Organizing Data Analysis Technique (ISODATA) module in ERDAS Imagine. ISODATA represents a fairly comprehensive set of heuristic procedures that have been incorporated into an iterative classification algorithm (ERDAS, 1994). ISODATA is self-Organizing because it requires relatively little human input. The ISODATA algorithm requires the analyst to specify the following criteria: (a) C-max which is the maximum number of clusters to be identified by the algorithm (e.g., 12 clusters) and (b) T which is the maximum percentage of pixels whose class values are

allowed to be unchanged between iterations. When this number is reached, the ISODATA algorithm terminates. For the study area, a maximum iteration of 25 with a convergence threshold of 0.95 was set using a X and Y skip factor of 1 to insure that the clustering algorithm processed all pixels.

The result of the unsupervised classification yielded a pseudo color five class GIS thematic map and provided the initial qualitative evaluation of the spectral characteristics of the digitized NAPP imagery as compared to the vegetation data previously mapped by Scott. The classification scheme for this thesis is developed by generalizing the existing vegetation data from Scott to 5 classes which coincide with the objectives of this study. For example, guided by the unsupervised classification, the detailed alpine vegetation data collected by Scott are generalized into five alpine vegetation habitat classes: (a) Moderately Drained Tundra Meadow, (b) Dry Meadow, (c) Exposed Fellfield/Moist Vegetation, (d) Exposed Fellfield, and (e) Moist Tundra Meadow. The sample sites are selected from Scott's field data, revisited during the GPS survey and compared to the five class thematic map in order to properly select the appropriate training areas for the supervised classification phase. The methodology for this research is based on the logical channel method to integrate the digitized NAPP and DEM data. Two supervised logical classification algorithms are employed: (a) linear discriminant functions and (b) maximum likelihood decision rules. Reference materials for training the classifiers include Scott's vegetation data, resource inventory maps, analog airphotos and field reconnaissance. The data gathered by the field reconnaissance are also used for the classification accuracy.

The logical channel method is used for the following reasons: (a) it has been used successfully in graduate thesis work aimed at general land cover classification (Franklin & Moulton, 1990) and (b) it is a basic method available on commercial image processing software for incorporating ancillary topographic data to compensate for topographic effect (Franklin & Moulton, 1990, Hutchinson, 1982).

Statistical classifications are accomplished using the linear discriminant analysis (LDA) method to generate linear discriminate functions from the field or training data. The functions are then used to classify the training data to determine the classification accuracy. The LDA is processed on a Pentium II based computer using Windows NT with the MathSoft's geostatistical software package S-PLUS. Originally devised by R. A. Fisher as a "sensible" way of distinguishing between groups, LDA is a method of classification that statistically distinguishes between two or more groups from a collection of discriminating variables. The discriminating variables measure the characteristics on which groups are expected to differ. The objective of LDA is to combine mathematically, the variables in a weighted, linear fashion, so the groups are forced to be as statistically distinct as possible (S-Plus 2000, 1996). The structure of the discriminant function can be written in the following form:

$$Y = a_1 x_1 + a_2 x_2 + \dots + a_n x_n$$

Where $x_1, x_2 \dots x_n$ are the variables

and $a_1, a_2 \dots a_n$ are coefficients used to determine a single value for Y.

A linear discriminant function takes an original set of measurements from a sample and transforms it into a single discriminant score. LDA therefore, reduces a multivariate problem to a linearly ordered situation (Davis, 1986).

Output from the LDA is in tabular form so interpretations consist of statistical comparisons between the collected field data and the digitized NAPP and DEM data sets, the discriminant functions and contingency tables of the percent correctly and incorrectly classified pixels. The contingency tables are used to construct error matrices as discussed by Congalton (1991). Total accuracy, errors of commission, errors of omission, and Kappa statistics are then reported from this information.

LDA is used to determine the statistical accuracy assessment of the classifications and to test the potential to reduce the number of variables for subsequent analysis and mapping. The number of variables is reduced so that the optimal discriminating power is maintained and redundant variables are eliminated from the analysis. This is done so a data set with a minimum number of variables can be used for input into the maximum likelihood classifier. The latter task is to illustrate the spatial distribution of the classification. The maximum likelihood classifier is run using ERDAS Imagine for Windows NT on a Pentium II based processor. Discriminant analysis, in general, is a process of dividing up n -dimensional space into k pieces such that the groups are as distinct as possible. While cluster analysis seeks to divide the observations into groups, discriminant analysis presumes the groups are known and seeks to understand what makes them different.

The maximum likelihood classification procedure requires three steps: (a) location of the training areas on the image, (b) generation of the class signatures, and (c) classification of the entire image. The field sites are located on the image using the GPS data collected during site reconnaissance for training area selection. Grey levels are then assigned and class signatures are generated for the training areas.

The class signatures are the probabilities used to classify each pixel into one of the given classes. Each pixel is put into the class for which it has the highest probability. The range of each class is defined as a hyperellipse surrounding the means of the classes. The algorithm used in ERDAS Imagine is the Mahalanobis minimum distance (ERDAS, 1994). If a pixel falls inside the hyperellipse of a class, a probability value is assigned to the class with the highest probability value. Conversely, if a pixel does not fall inside any hyperellipse or at least one band exceeds the limits of the hyperellipse, the pixel is assigned to the null class. The results from the maximum likelihood classification are written to a pseudo-color image channels and colors are reassigned to enhance the display. The supervised classification land cover map is illustrated in Appendix B.

CHAPTER 4

ANALYSIS AND RESULTS

This chapter describes the spectral relationships among the digitized NAPP channels using statistical and graphical feature selection of the digitized NAPP imagery, field topography and DEM data sets. In order to discover the extent to which NAPP imagery can be used to classify alpine vegetation a transformed divergence statistic and co-spectral plot algorithm were used to test the correlation of the digitized NAPP channels. Bivariate relations among the field and digitized NAPP variables were evaluated to test for variable similarity and to aid in the prediction of what results can be expected from discriminant function classification.

Discriminant function analysis was used to conduct the statistical classifications of the data sets. The field data were classified to determine the ability of the data to represent the surface cover of the study area. Finally, the digitized NAPP and DEM data sets were combined to determine classification accuracy of the complete data set and to determine the extent to which these data sets improved the accuracy of the classification.

Methods of feature selection were used to quantitatively and qualitatively select which subset of bands (or features) provides the greatest degree of separability between any two data classes. The basic problem of spectral pattern recognition is that, given a spectral distribution of data in bands of remotely sensed data, a discrimination technique must be used that allows separation of the major land cover categories with a minimum of error and a minimum number of bands. These statistical methods are used to reduce the amount of redundant data. When data overlaps, the appropriate decision rule can be

used. In the classification of remotely sensed data, we are concerned with two types of error: (a) that a pixel may be assigned to a class to which it does not belong (an error of commission), and (b) that a pixel is not assigned to its appropriate class (an error of omission). Evaluating the separation (correlation) between variables and classes is used here to help predict, understand, and explain why such errors occur when using digitized NAPP and topographic data sets.

Signature Evaluation

Transformed Divergence

Divergence is one of the first measures of statistical separability used in machine processing of remote sensor data. It is widely used as a method of feature selection (Mausel, Kamber, & Lee, 1990). This statistic gives an exponentially decreasing weight to increasing distances between classes and scales the divergence values to lie between 0 and 2000. This demonstrates which bands yield the greatest separability when taken 1, 2, or 3 at a time. It is more useful; however, to calculate divergence with single or paired bands of digitized NAPP imagery for discrimination among all classes of interest.

The transformed divergence relationships can indicate if information is shared between the variables in a data set. If information is similar between variables within a dataset, then some of the variables may be redundant. For example, if the digitized NAPP channels are highly correlated then similar information is shared among the channels; therefore, some of the channels may be eliminated from further analysis, which may produce similar results to the full data set. This can be useful when determining if the surface cover of a study area is well represented by the digitized NAPP data. If the

surface cover, as represented by accurate ground data, correlated highly with the digitized NAPP data, then high classification accuracies could be expected.

The bivariate relationships can indicate if information is shared between variables in a dataset or between variables in different data sets. If information is similar between variables within a dataset, then some of the variables may be redundant. If correlations between variables of different data sets are high, then variables from one data set can be used to predict the other. Weak to moderate correlations between variables of two predictor data sets may suggest the data sets contain different information that will improve the success of further analysis if used together. For example, moderate correlations between the digitized NAPP and DEM data sets could suggest that classification accuracies will be highest when the two data sets are integrated into a classification rather than used separately (Franklin & Ledrew, 1984). An analysis of the bivariate relationships between the variables is employed to test suitability of the data sets for use in the discriminant function classification.

As noted above, transformed divergence measures the between-class separation between data sets. In this section, the transformed divergence of the three digitized NAPP bands (or channels) and the class pairs as decided by the ground reference data and the unsupervised classification are examined. This is done in attempt to understand the variations of the NAPP channels as compared to the class pairs. The correlation between the digitized NAPP and derived class pairs for the 256 “known” sample pixels are presented in the Tables 12-14. The important relationships between

Table 12

Transformed Divergence Signature Separability Listing Using Bands: 1 2 3 Taken 3 at a Time

Bands	Average	Minimum	Separability Listing Class Pairs									
			1:2	1:3	1:4	1:5	2:3	2:4	2:5	3:4	3:5	4:5
1 2 3	1971	1726	2000	2000	2000	1726	2000	2000	2000	1980	2000	2000

Note. Normalized probability is 0.2000. Class 1 = Moderately Drained Tundra Meadow; Class 2 = Dry Meadow; Class 3 = Exposed

Fellfield/Moist Vegetation; Class 4 = Exposed Fellfield; Class 5 = Moist Tundra Meadow. Band 1 = Red; Band 2 = Green; Band 3 = Blue.

Table 13

Transformed Divergence Signature Separability Listing Using Bands: 1 2 3 Taken 2 at a Time

Bands	Average	Minimum	Separability Listing Class Pairs										
			1:2	1:3	1:4	1:5	2:3	2:4	2:5	3:4	3:5	4:5	
1 2	1989	1887	2000	2000	2000	1887	2000	2000	2000	2000	2000	2000	2000
1 3	1998	1982	2000	2000	2000	1882	2000	2000	2000	2000	2000	2000	2000
2 3	1945	1451	2000	2000	2000	1451	2000	2000	2000	1998	2000	2000	2000

Note. Normalized probability is 0.2000. Class 1 = Moderately Drained Tundra Meadow; Class 2 = Dry Meadow; Class 3 = Exposed Fellfield/Moist Vegetation; Class 4 = Exposed Fellfield; Class 5 = Moist Tundra Meadow. Band 1 = Red; Band 2 = Green; Band 3 = Blue.

Table 14

Transformed Divergence Signature Separability Listing Using Bands: 1 2 3 Taken 1 at a Time

Bands	Average	Minimum	Separability Listing Class Pairs									
			1:2	1:3	1:4	1:5	2:3	2:4	2:5	3:4	3:5	4:5
1	1936	1639	2000	1997	2000	1961	2000	2000	2000	1639	1839	1926
2	1984	1844	2000	2000	2000	1844	2000	2000	2000	2000	2000	2000
3	1862	624	2000	2000	2000	624	2000	2000	2000	1998	2000	2000

Note. Normalized probability is 0.2000. Class 1 = Moderately Drained Tundra Meadow; Class 2 = Dry Meadow; Class 3 = Exposed Fellfield/Moist Vegetation; Class 4 = Exposed Fellfield; Class 5 = Moist Tundra Meadow. Band 1 = Red; Band 2 = Green; Band 3 = Blue.

variables that help explain the digitized NAPP spectral response are discussed in the following sections.

A transformed divergence value of 2000 suggests excellent between-class separation, while below 1700 is poor. The class separability of the class pairs against all three bands (RGB) for the Roaring Fork Study area indicates the overall average spectral separability is 1971 (Table 12). Normally, there is no need to compute the divergence using all three bands as this represents the totality of the data set. In the case of digitized NAPP imagery, however, it was computed as a baseline for reference. Class Pairs 1 and 5 (Moderately Drained Tundra Meadow and Moist Tundra Meadow) and 3 and 4 (Exposed Fellfield/Moist Vegetation and Exposed Fellfield) indicate strong to weak correlations with individual figures of 1726 and 1980, respectively. Under the parameters of the transformed divergence algorithm, this is considered acceptable results. This indicates the three digitized NAPP bands are highly correlated with respect to classes 1 (Moderately Drained Tundra Meadow) and 5 (Moist Tundra Meadow). Thus, some (or all) of the channels may be redundant. Results of the correlations between landcover variables indicate close association between vegetation and mineral data in the study area. The analyses of the class pairs in relation to all three digitized NAPP channels show a strong separability value of 2000. This value indicates weak correlations for all class pairs except for classes 1:5 (Moderately Drained Tundra Meadow and Moist Tundra Meadow) and 3:5 (Exposed Fellfield/Moist Vegetation and Exposed Fellfield). The variables of Moderately Drained Tundra Meadow and Moist Tundra Meadow have moderate to strong negative correlation. A negative correlation indicates there is a

dominant control mechanism between the class pair 1:5 (Moderately Drained Tundra Meadow and Moist Tundra Meadow) and the three digitized NAPP channels. In the longer wavelengths of the near-infrared portion of the spectrum (700-1350 nm), both reflectance and transmittance are high while absorptance is very low. Color infrared films are sensitive to ultraviolet, visible, and infrared radiation to approximately 900 nm. Though water content is very different in these two alpine habitats, in near infrared wavelengths the primary control mechanism is moisture and internal leaf structures resulting in the strong correlation. Soil moisture, organics, and particle size are potential control mechanisms in these wavelengths; however, soil profiles were not described for this research.

The mineral content of the class pair of 3:4 (Exposed Fellfield/Moist vegetation and Exposed Fellfield) indicates a weak correlation resulting in an acceptable between class separation value of 1980. This value is driven by the moist vegetation component while being lowered by similar mineral characteristics.

Table 13 illustrates band pairs taken 2 at a time in relationship to class pairs. The table provides additional information regarding the spectral characteristic of digitized NAPP imagery. Band combinations 1:2, 1:3, and 2:3 result in average between-class separability values 1887, 1882, and 1451, respectively, for the class pair of 1:5 (Moderately Drained Tundra Meadow and Moist Tundra Meadow). Band combinations 1:2 and 1:3 indicate moderate to good between-class separation. Bands 2 and 3 provide the highest correlation with the class pair 1:5 (Moderately Drained Tundra Meadow and Moist Tundra Meadow) indicating that spectral characteristics of these two bands contain

too much redundant or overlapping information to be used successfully. Class pair 3:4 (Exposed Fellfield/Moist vegetation and Exposed Fellfield) indicates a minimal increase in correlation in relationship to Bands 2 and 3, however, the separability value of 1998 is considered negligible. According to the transformed divergence statistics for Bands taken 2 at a time, Bands 1 and 3 provide the best minimum and average signature separability discrimination for the class combinations used in this study.

The signature separability listing in Table 14 illustrates the transformed divergence statistics using digitized NAPP imagery Bands 1, 2, and 3 taken 1 at a time. This signature separability listing provides the most information on the spectral characteristics of the digitized NAPP imagery. The average individual band separation value ranged from 1862 to 1984, while minimum separability ranged from 624 to 1844. Band 2 provides the best overall average and minimum separability values of, 1984 and 1844, respectively. Both statistical values fall within the guidelines of moderate class separation. Band 2 indicates an increase in correlation of class 1:5 (Moderately Drained Tundra Meadow and Moist Tundra Meadow). Otherwise, Band 2 yields a value of 2000 which suggests excellent between-class separation of all other class pairs.

Band 1 shows increased correlation between class pairs 1:3, (Moderately Drained Tundra Meadow and Exposed Fellfield/Moist Vegetation), 1:5 (Moderately Drained Tundra Meadow and Moist Tundra Meadow), 3:4 (Exposed Fellfield/Moist Vegetation and Exposed Fellfield), 3:5 (Exposed Fellfield/Moist Vegetation and Moist Tundra Meadow), and 4:5 (Exposed Fellfield and Moist Tundra Meadow). The minimum statistical value for Band 1 is 1639 for the class pair 3:4 (Exposed Fellfield/Moist

Vegetation and Exposed Fellfield). This value suggests that Band 1 should not be used alone for the analysis of Exposed Fellfield/Moist Vegetation and Exposed Fellfield.

However, as noted in Table 12, where bands are taken 2 at a time, Band 1 when combined with Band 3 yields excellent between-class separation and is suggested as the best overall band combination for these alpine vegetation habitats including the class pair of 3:4 (Exposed Fellfield/Moist vegetation and Exposed Fellfield).

Band 3 suggests a moderate signature separability value at 1862. This average value is skewed by the outlier for the 1:5 (Moderately Drained Tundra Meadow and Moist Tundra Meadow) class pair value of 624. Excluding the 1:5 (Moderately Drained Tundra Meadow and Moist Tundra Meadow) class pair value, Band 3 yields excellent signature separability with an average value of 1999.

Cospectral Feature Space Plots

The transformed divergence quantitatively demonstrates which bands and band combinations provides the best signature separability. Feature space plots provide useful visual between-class separability information (Jensen & Toll, 1982) and provide the actual insight into the between band correlation. The plots are generated using the mean and standard deviations of the training class statistics for each class band. They consist of a 256 x 256 matrix (0 to 255 in the x-axis and 0 to 255 in the y-axis). In Figures 15-17 the training class statistics for the five Roaring Fork Mountain alpine vegetation habitat classes are portrayed in this manner and draped over the feature space plot of the digitized NAPP Bands 1:2; 1:3; and 2:3. The lower and upper limits of the two-dimensional parallelepipeds (rectangles) were obtained using the $\pm 1\sigma$ of each band of

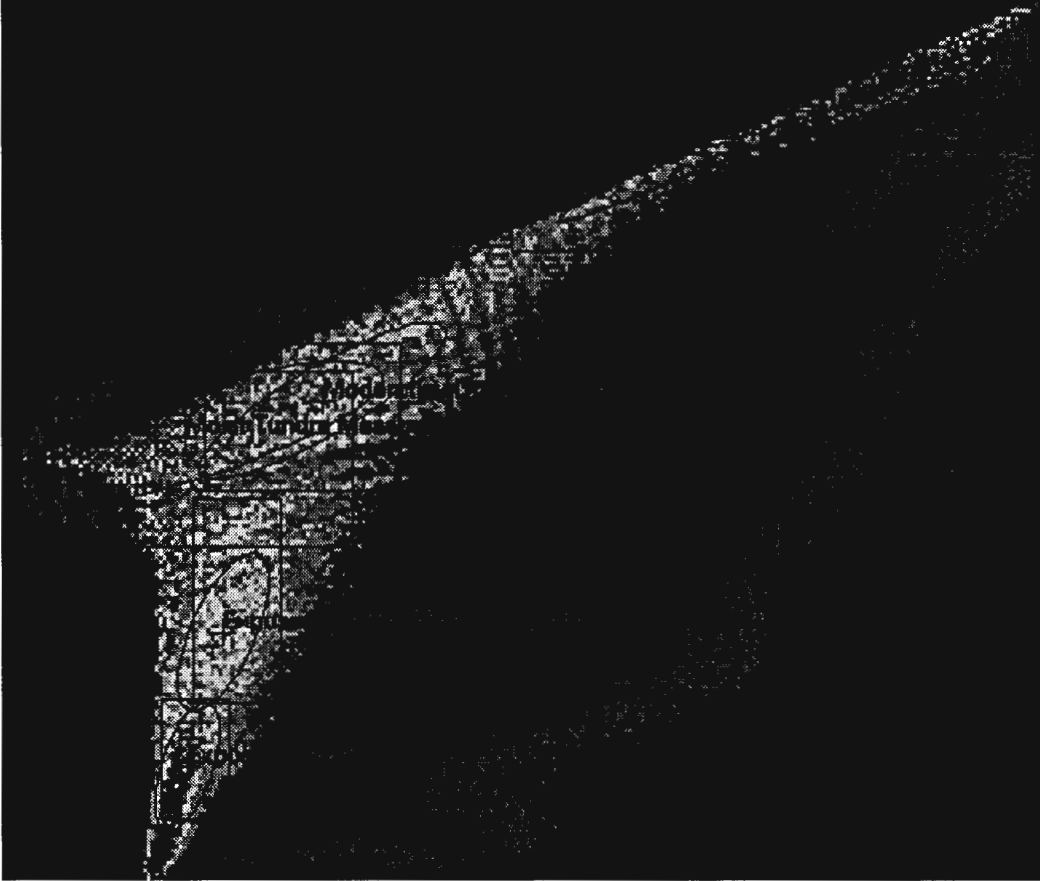


Figure 14. Plot of the Roaring Fork Mountain, Wyoming, digitized NAPP training statistics for five classes measured in Bands 1 and 3 displayed as co-spectral parallelepipeds. The upper and lower limit of each parallelepiped is ± 1 standard deviation.

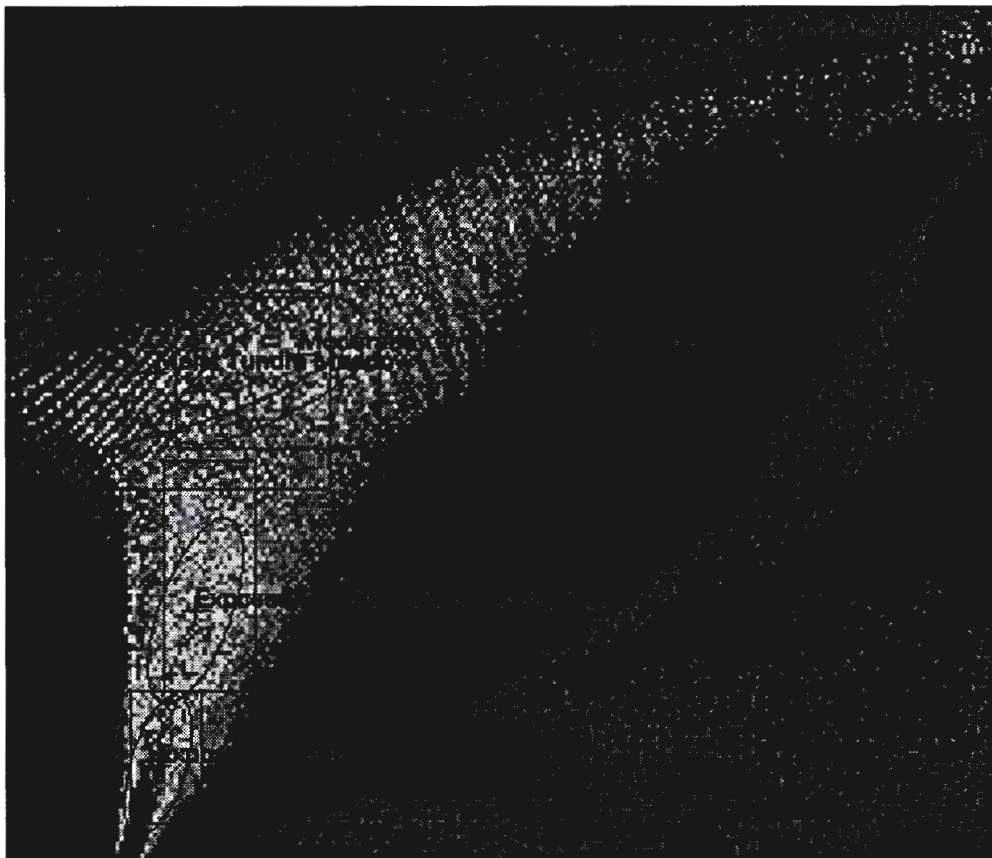


Figure 15. Plot of the Roaring Fork Mountain, Wyoming, digitized NAPP training statistics for five classes measured in Bands 1 and 2 displayed as co-spectral parallelepipeds. The upper and lower limit of each parallelepiped is ± 1 standard deviation.

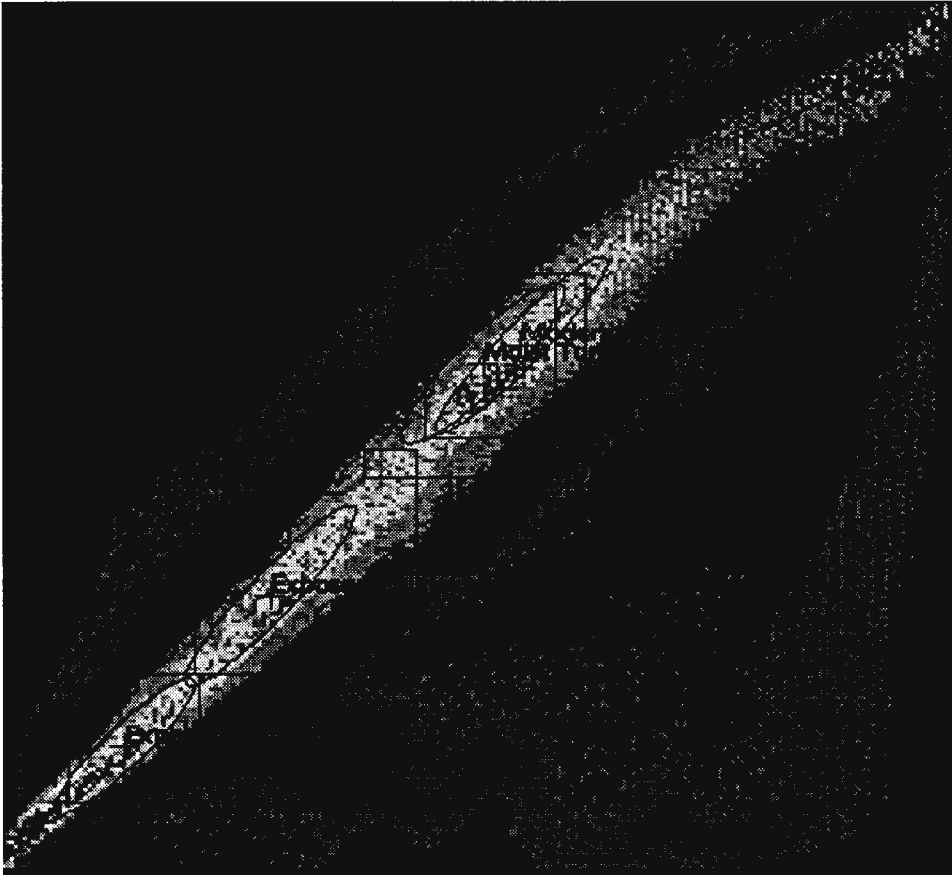


Figure 16. Plot of the Roaring Fork Mountain, Wyoming, digitized NAPP training statistics for five classes measured in Bands 2 and 3 displayed as co-spectral parallelepipeds. The upper and lower limit of each parallelepiped is ± 1 standard deviation.

each class. There would be confusion between class pairs 1 (Moderately Drained Tundra Meadow) and 5 (Moist Tundra Meadow) if only Band 3 data were used to classify the scene. The separation of those class pairs become more distinct when including Bands 1 and 2. The classes of Moderately Drained Tundra Meadow and Moist Tundra Meadow mirror the results of the transformed divergence algorithm. The high correlation between these two classes can be a result of the low discrimination characteristics of the digitized NAPP imagery or the lack of appropriate training data collected in the field. Normally, water or moisture is a robust enough of control that good between-class separability can usually be expected. All three plots share some similarity, however, with the techniques used in discriminate analysis redundant information can be placed in its appropriate class.

Bivariate Correlation

In this section, the bivariate correlations between the measured variables and the digitized NAPP channels are examined. Bivariate correlation (also known as the product-moment coefficient of correlation) measures or estimates the linear association of two variables (Davis, 1986). This is done in order to describe the variation of the NAPP channels contributed by the surface cover as represented by the field variables.

Correlations between NAPP channels indicate that some channels are correlated and most likely contain redundant data. The correlation coefficients between each NAPP channel, and topographic and landcover variables for the sites visited in the field are presented in Table 15.

For the three digitized NAPP color channels correlations range from 0.30 to 0.90. The weakest correlation (0.30) is between NAPP Channel 1 (Red) and NAPP Channel 2

Table 15

Bivariate Correlation Matrix

Variable	Bivariate Correlation Matrix										
	Band 1 (Blue)	Band 2 (Green)	Band 3 (Red)	Elevation	Slope	Incidence	MDTM	DM	EF/MV	EF	MTM
Band 1 (Blue)	1.00										
Band 2(Green)	0.30	1.00									
Band 3 (Red)	0.32	0.90	1.00								
Elevation	0.41	0.55	0.52	1.00							
Slope	0.24	0.39	0.44	0.62	1.00						
Incidence	0.22	0.26	0.36	0.40	0.66	1.00					
MDTM	0.23	0.32	0.26	0.39	0.43	0.33	1.00				
DM	0.14	0.20	0.18	0.38	0.39	0.27	0.16	1.00			
EF/MV	0.32	0.31	0.28	0.42	0.52	0.41	0.21	0.17	1.00		
EF	0.34	0.32	0.37	0.40	0.28	0.23	0.14	0.19	0.94	1.00	
MTM	-0.04	-0.16	-0.07	-0.08	-0.49	-0.22	0.43	0.11	0.09	-0.11	1.00

(Green). The strongest correlation (0.90) exists between NAPP Channel 2 (Green) and NAPP Channel 3 (Blue). Results of correlations between land cover classes indicate some close habitat associations in the study area. The significant positive correlations between the topographic variables possibly exist because the variables of slope and aspect are related to elevation. For example, slope can be extracted from elevation, and incidence can be calculated from slope and aspect, both derivatives of elevation (Jensen, 1996). Other factors might also explain these relationships. The correlation between elevation and slope (0.62) could be explained by the assumption that areas modified by glacial erosion generally increase in slope angle with increasing elevation (Franklin & Ledrew, 1984). The correlation between slope and incidence (0.66) could partially be explained by higher slope angles resulting in higher incidence values. A number of moderate correlations are found between ground cover and topographic variables. The correlations of elevation with MDTM (0.39), DM (0.38), EF/MV (0.42), EF (0.40), and MTM (-0.08) indicate altitudinal control of these variables. The variable associated with a decrease in alpine vegetation cover as elevation increases and the non vegetated variables such as bare rock increase where alpine vegetation is limited.

Franklin and Moulton (1991) also found elevation to be negatively correlated with alpine vegetation and positively correlated with vegetated and non-vegetated surfaces in mountainous study areas in North America. The positive correlation between elevation and slope is reflected in the relationship between slope and land cover classes where the direction of the correlation of elevation with these variables is generally the same for slope. The highest correlations between slope and the land cover variables are MDTM

(0.43), DM (0.39), and EF/MV (0.52). The moderate positive correlations between slope and the MDTM (0.43), DM (0.39), EF/MV (0.52) could reflect this association with 15° to 35° slope angles (Franklin & Moulton, 1991). The non-vegetated EF class also tends to occur on steeper slopes. The moderately negative relationships between slope and MTM is negatively correlated with MTM (-0.49), possibly because water generally does not collect on high slope angle. The exceptions are the numerous high angle seeps located in the study area where lush vegetation is associated with thin drainage networks. The spectral resolution of digitized NAPP imagery was unable to distinguish these features.

The relationship between incidence and the land cover variables is similar to that of elevation and slope. The highest correlations are between incidence and EF/MV (0.41), MDTM (0.33), and DM (0.27). Incidence is calculated from the position of the sun and sky at the time the image was acquired (altitude and azimuth) and specific slope and aspect values for each sample site. The highest incidence values are, therefore, southerly facing with aspect values equivalent to the solar azimuth and slope values equivalent to the solar elevation. For the digitized NAPP image used here, the maximum values will occur on 15 to 25° slopes facing approximately a 270° azimuth. Conversely, low incidence values will occur on the lower southeasterly portions of the slopes and valley bottom. The slopes with high incidence values should be associated with dryer moisture regimes than those with low incidence values because the west facing slopes receive higher solar radiation levels and, thus, higher soil temperatures. Therefore, landcover variables that are positively correlated with incidence should be dryer and

those with negative correlations, wetter. In the correlations above, the negative correlations are the EF and MTM (-0.22). Higher incidence values also occur where there is exposed rock surfaces and very dry soil which normally indicates restricted plant growth.

Weaker correlations occur between the land cover variables and the digitized NAPP channels. Negative correlations exist between the MTM variable and the NAPP band response ranging from -0.04 to 0.16. This negative correlation indicates that, as the percent coverage of moist landcover increases, the amount of light reflected decreases due to absorption. This implies that wetter areas reflect less radiation than do dryer areas. There also could be differences in reflectance values recorded by the Aerochrome 2443 film for this landcover type. This is consistent with Franklin and Moulton (1991) who found that alpine wetland or highly saturated alpine vegetation can be negatively correlated with near-infrared sensor data. There are positive correlations between digitized NAPP bands and vegetated land cover classes that range from 0.14 to 0.37. This is a result of the reflective characteristics of dryer herbaceous vegetation in the near infrared portion of the spectrum as sensed by NAPP imagery (Jensen, 1996). As expected, the Exposed Fellfield class is moderately reflective, thus, positively correlated with all digitized NAPP bands with a range from (0.14 to 0.28).

The range of correlation values between elevation and spectral channel are from 0.41 to 0.55 with the highest correlations in the green Channel (2). The ranges of correlations are in a agreement with Smith (1996) for the green Channel (2). The positive correlations for this study area can be explained by the elevation of the landcover

variables. Surfaces that absorb radiation are generally located on lower slopes than surfaces with high reflective properties. For example, Wet Moist Tundra Meadow (a high absorber of radiation in all spectral channels) is located in areas of “steps” where meltwater and local precipitation collect. Herb vegetation and bare rocks, which have greater reflectance in all spectral channels, occur on steeper slopes and generally higher elevations. The correlation between incidence and digitized NAPP response is positive for all bands in the range from 0.22 to 0.36. This correlation can be explained by the slopes facing the azimuth of the sun reflecting more directly to the camera during image acquisition. This effect is discussed in detail by Holben and Justice (1981).

Correlations between the surface cover, digitized NAPP variables, and topographic variables help to describe associations among the sets of variables here. Examination of these statistics and comparisons to the literature indicate that the data set will work with the discriminant analysis technique. For example, the strong correlations among the digitized NAPP variables indicate redundancy in the data, so at least one of the channels could be removed before the maximum likelihood classification is attempted.

Moderate correlations among the topographic channels indicate some similarities are related but probably not redundant, since the highest correlation is 0.66 (between elevation and slope). This would indicate that the topographic data may bring more information into subsequent classification procedures. The weak to moderate correlations from -0.04 to 0.37 suggest there is information available in the digitized NAPP channels that represent the surface cover of the study area. However, the weak

correlations indicate the variation of the surface cover is not totally captured by the NAPP imagery. These bivariate relationships indicate that an integrated data set of three digitized NAPP channels and the three topographic variables (elevation, slope, and incidence) bring more information in the supervised classification than the digitized NAPP by itself. In order to test this interpretation, the discriminant function classification procedure was applied to this data.

Discriminant Analysis Classification and Accuracy Assessment

This section describes the results of the linear discriminant analysis, which is a method of automated classification based on statistical analysis of the data (Davis, 1986). Discriminant analysis is designed to investigate the power of the variables to correctly classify the data and to test the hypothesis that integrating the remotely sensed data (the digitized NAPP) and a DEM data set will provide a better classification than either data set alone. Information from training pixels is used to generate discriminant functions. The functions are then used to classify the original training pixels or additional pixels. In this study the 256 pixels are used to train the discriminant function. The same 256 pixels subsequently are classified based on the generated functions. Past research has shown this technique overestimates the classification accuracy, but that it can be used to determine differences in function performance (Davis, 1986). Accuracy of the classifications are determined by the use of error matrices that include overall accuracy, omission of error, commission of error, and Kappa statistics.

Recall that there are five broad land cover classes that describe the vegetated and non-vegetated surfaces of the study area (Table 10). Each sample site or pixel visited in

the field is assigned to one of these classes for each of three data sets: (a) field topographic data, (b) digitized NAPP data, and (c) DEM data. These data sets are input into the linear discriminant analysis using the following combinations: (a) digitized NAPP data, (b), DEM data, (c) digitized NAPP + elevation (DEM), (d) digitized NAPP + slope (DEM), (e) digitized NAPP + incidence, and (f) digitized NAPP + DEM data. These combinations are used to determine how well the variables and the discriminant function describe the ability of digitized NAPP to discriminate the classes and the increase in discriminating power of combining the digitized NAPP and DEM data sets. In the linear discriminate procedure, a mean vector and co-variance matrix characterizes each class. The assumptions made for this procedure are (a) multivariate normality and (b) homogeneous co-variance matrices.

Digitized NAPP Error Matrix

The digitized NAPP data set consists of three channels (Red, Green, and Blue) representing the visible green, visible red, and near infrared portions of the electromagnetic spectrum (as originally captured by the Kodak Aerochrome 2443 film). The discriminant function classification of the three channels is discussed in this section.

The digitized NAPP has an overall classification accuracy of 76.17% for the five classes (Table 16; error matrix). The range for individual class accuracies (error of omission) varies from 31% for Dry Meadow to 97% for Moderately Drained Tundra Meadow. These classification accuracies illustrate the success of the classification but do not suggest where the problems of confusion between classes might occur. Table 16 (error matrix) contains the error matrix that illustrates the misclassification between

classes. The pixels from Moderately Drained Tundra Meadow have a classification success of 89.9% or a 10.1% error of omission. Although 89.9% of Moderately Drained Tundra Meadow pixels were correctly identified as Moderately Drained Tundra Meadow only 71.6% of the areas called Moderately Drained Tundra Meadow are actually Moderately Drained Tundra Meadow on the ground (error of commission). A closer look reveals some confusion between classes. Moderately Drained Tundra Meadow has pixels that are misclassified into Dry Meadow, and Exposed Fellfield/Moist Vegetation, with the largest amount into the class of Moist Tundra Meadow resulting in confusion among classes. Similarly, a moderate amount of misclassified pixels from Moist Tundra Meadow are misclassified into Moderately Drained Tundra Meadow along with Exposed Fellfield/Moist Vegetation and Exposed Fellfield. This indicates there is poor discrimination between Moderately Drained Tundra Meadow and Moist Tundra Meadow. Earlier signature evaluation of the digitized NAPP channels also indicated spectral confusion between these two classes. The misclassification of pixels from Moist Tundra Meadow into Exposed Fellfield is attributed to confusion in the spectral response of the digitized NAPP image rather than error in the data collection. The misclassified pixels of Exposed Fellfield/Moist Vegetation into both Dry Meadow and Exposed Fellfield is attributed to confusion between similar reflective properties as seen by areas of Fellfield and well drained or very dry alpine soils almost always located on slopes. The same results are seen with Exposed Fellfield. Misclassification within the digitized NAPP data set will be the result of spectral discrimination characteristics giving similar spectral signatures.

Table 16

Error Matrix of the Classification Map of Roaring Fork Mountain, Wyoming Derived from Digitized NAPP Data

Classification	Reference					Row Total	
	MDTM	DM	EF/MV	EF	MTM	195	256
MDTM	57	3	1	0	8		
DM	0	4	2	0	0		
EF/MV	0	6	71	3	1		
EF	0	0	6	31	2		
MTM	2	0	2	4	53		
Column Total	59	13	82	38	64	195	256
Overall Accuracy = $195 / 256 = 76.17\%$					Khat = 68.4%		

Note. MDTM = Moderately Drained Tundra Meadow; DM = Dry Meadow; EF/MV = Exposed Fellfield/Moist Vegetation;

EF = Exposed Fellfield; MTM = Moist Tundra Meadow.

As part of the error evaluation a KAPPA analysis was performed. A discrete multivariate technique, KAPPA yields a Khat statistic that is a measure of agreement or accuracy (Congalton, 1991). Congalton (1998) suggests that in order to glean as much information from the error matrix the Khat statistic be computed. The computation of the Khat statistic is computed with the following equation:

$$K_{hat} = \frac{N \sum_{i=1}^r \chi_{ii} - \sum_{i=1}^r (\chi_{i+} \times \chi_{+i})}{N^2 - \sum_{i=1}^r (\chi_{i+} \times \chi_{+i})}$$

Where $N = 256$

$$\sum_{i=1}^r \chi_{ii} = (53 + 4 + 66 + 28 + 44) = 195$$

$$\sum_{i=1}^r (\chi_{i+} \times \chi_{+i}) = (74 \times 59) + (6 \times 13) + (79 \times 82) + (41 \times 38) + (56 \times 64) = 16,064$$

$$K_{hat} = \frac{256(195) - 16,064}{256^2 - 16,064} = \frac{55,296 - 16,064}{65,536 - 16,064} = \frac{33,856}{49,472} = 68.4\%$$

The overall classification accuracy of the error matrix 76.17%, while the Khat is 68.4%. The results are different because the Khat statistic incorporates the major diagonal and excluded the omission and commission errors. The Khat computation incorporates the off-diagonal elements as a product of row and column marginals is used to determine if the results presented in the error matrix are significantly better than the random result. The Khat statistic was included in this study as a means of comparison

between the integrated data set of digitized NAPP channels and DEM data and future remote sensing investigations.

The classification accuracies from the digitized NAPP data compares with two studies in similar mountainous terrain using the same methodology, however, using Landsat TM data instead of the digitized NAPP imagery. These studies had overall classification accuracies of 60% and 77% (Franklin & Moulton, 1990; Franklin & Wilson, 1991).

Evaluating Field and DEM Topographic Data

The field topographic data as provided by Scott and DEM topographic variables were classified and assessed for their individual and overall mean accuracies prior to integrating the DEM and digitized NAPP data. This was done to insure that the DEM variables could be used in place of field topographic data for this study and future studies beyond this site. This is important because detailed field topographic data, such as the data collected by Scott, may not always exist.

The DEM contains the full 5 class test pixel data set for all three variables but the DEM data required spatial resampling before being integrated with the other data sets. Using a USGS DRG draped over the USGS DEM, I plotted additional elevation points to increase the spatial resolution of the 30 meter DEM to 8.5 meter per pixel resolution. Resampling the pixel resolution of the DEM was done to more adequately match the 1 meter pixel resolution of the digitized NAPP imagery.

Table 17 summarizes the classification accuracies obtained from the field topographic variables and DEM topographic variables. Included are individual variable

Table 17

Summary of Classification Accuracies of the Field and DEM Topographic Variables are Percent Accuracy by Class

Class	Field Topographic Variables				DEM Topographic			
	Elev.	Slope	Incid.	All	Elev.	Slope	Incid.	All
MDTM	6.0	59.8	24.6	48.5	67.6	0.0	0.0	22.1
DM	28.4	50.5	0.0	11.0	0.0	9.2	0.0	15.5
EF/MV	27.3	34.1	12.4	27.0	4.5	33.7	6.9	10.6
EF	43.2	62.7	36.1	53.6	52.1	49.4	48.2	56.6
MTM	22.9	55.2	22.8	32.4	23.7	45.3	14.6	37.9
Mean	25.56	52.46	19.18	34.5	29.58	27.52	13.94	28.54

Note. Elev = Elevation; Incid = Incidence. MDTM = Moderately Drained Tundra Meadow; DM = Dry Meadow; EF/MV = Exposed Fellfield/Moist Vegetation; EF = Exposed Fellfield; MTM = Moist Tundra Meadow.

classifications and the three variables used in combination. The overall classification accuracy for all three variables is 39.2%. The accuracy range is from 11.8% for Dry Meadow to 88% for Exposed Fellfield. Classification accuracies for Moderately Drained Tundra Meadow, Exposed Fellfield/Moist Vegetation, and Moist Tundra Meadow are 62.2%, 28.1% and 47.8% respectively. These moderate to high classification accuracies indicate the topographic variables contain important information that describe the characteristics of the Roaring Fork Mountain study area.

The overall classification accuracy for individual topographic variables is highest for slope (52.46%) followed by elevation (25.56%) and incidence (19.18%). This indicates that slope is the most important topographic variable. When the classifications of the field topographic data and DEM data sets are compared, most accuracies are similar. The overall classification accuracy for all three variables of the DEM data set is 28.54%. The overall classification accuracy is 5.96% lower than the field data. This is expected because the field data was measured directly in the field, where as the DEM was originally 30 meters and resampled down to 8.5 meters per pixel resolution (which increases the potential for induced error). However, there is not a significant difference between the overall accuracies of the topographic data set and DEM data set. Thus, DEM topographic then can be integrated with the digitized NAPP image. The highest overall classification accuracy for individual topographic variables is for elevation (29.58%) followed up by slope and incidence at 27.52% and 13.94%. This indicates that all three topographic variables are equally important overall. The importance of the variables is carried on into the discriminant function classification using the integrated data set of the digitized NAPP and topographic variables.

Evaluation of Digitized NAPP and DEM Topographic Data

The integrated data set that includes digitized NAPP and DEM variables contains the three color channels and the three topographic variables. The increase in classification accuracies gained by adding individual topographic variables and the DEM data set to the digitized NAPP data set are examined. Table 18 contains the individual and overall classification mean accuracy of different combinations of the integrated set.

Table 18

Summary of Classification Accuracies of the Digitized NAPP Channels 1-3 and the DEM Data Set

Class	Percent of Accuracy by Class (Omission Error)				
	Digitized NAPP	Digitized NAPP + Elevation	Digitized NAPP + Slope	Digitized NAPP + Incidence	Digitized NAPP + DEM
MDTM	89.9	73.6	72.9	69.9	96.7
DM	30.7	78.9	62.6	68.3	30.7
EF/MV	80.4	62.2	78.3	45.7	86.5
EF	73.6	77.3	88.8	67.5	81.5
MTM	68.7	72.9	73.7	66.2	82.8
Mean	68.66	72.98	76.70	63.52	75.64

Note. Elev = Elevation; Incid = Incidence. MDTM = Moderately Drained Tundra Meadow; DM = Dry Meadow; EF/MV = Exposed Fellfield/Moist Vegetation; EF = Exposed Fellfield; MTM = Moist Tundra Meadow.

The individual classes are compared to the individual topographic variables in order to identify the strengths of each variable in the overall classification accuracy.

The addition of incidence to the digitized NAPP data set produced a 5.14% overall decrease in classification accuracy from 68.66% to 63.52%. Moderately Drained Tundra Meadow received the only increase in accuracy by 1.24 %. The remaining classes all received decreases in accuracy by 0.05% to 23%.

The addition of elevation to the digitized NAPP data set increased accuracy by 4.32% overall to 72.98%. Moderately Drained Tundra Meadow increased the greatest from 30.7% to 78.9% while classes Exposed Fellfield and Moist Tundra Meadow increased 3.7% and 4.2% respectively. The classification of digitized NAPP + elevation resulted in unexpected decreases in individual class accuracies for both Moderately Drained Tundra Meadow (16.3%) and Exposed Fellfield/Moist Vegetation (18.2%). Differences in spatial resolution of the digitized NAPP image and the DEM data resulted in the possibility of increased error.

The addition of slope to the digitized NAPP data set increased accuracy by 8.04% to 76.70%. The accuracies of classes Dry Meadow, Exposed Fellfield, and Moist Tundra Meadow increased by 31.9% to 15.2% and 5% respectively. Moderately Drained Tundra Meadow decreased by 17% while class Exposed Fellfield/Moist Vegetation decreased by 2.1%.

The addition of all three topographic variables to the digitized NAPP image data set increased classification accuracy by 6.98% overall to 75.64%. The greatest increase for individual classes is for Moist Tundra Meadow at 14.1%. Moderately Drained Tundra Meadow, Exposed Fellfield/Moist Vegetation, and Exposed Fellfield also received increases between 5.1% and 7.9%. When individual topographic variables were applied to Dry Meadow, the increase in accuracy ranged from 31.9% to 48.2%. However, when the three combined topographic variables are applied to the digitized NAPP imagery, the number of misclassified pixels remain equivalent to the accuracy obtained with digitized

NAPP imagery alone (30.7%). This amount can be attributed to insufficient ground data when all three topographic variables are taken into account.

Integrated Digitized NAPP and DEM Error Matrix

The error matrix for the integrated data set classification is presented as Table 19. The addition of the three variables reduces the number of misclassified pixels by 70% (from 60 to 42). Remaining misclassified pixels (36.6%) are from within Moderately Drained Tundra Meadow. The majority of these misclassified pixels are error of commission and error of omission of the Moderately Drained Tundra Meadow class. This suggests that this class is poorly represented by both the digitized NAPP and DEM data sets even though the individual class accuracy is high. The misclassified pixels are most likely the result of poor signature discrimination of the digitized NAPP imagery.

The number of misclassified pixels for Exposed Fellfield/Moist Vegetation was reduced from 24 to 21. The decrease occurred with Exposed Fellfield indicating an increase in discriminating ability when the topographic variables of a DEM are included. The misclassified pixels of Exposed Fellfield are reduced by 16.6% from 18 to 15. The increase in accuracy occurred in related Exposed Fellfield/Moist Vegetation. The increase indicates the need for the topographic variables. Moist Tundra Meadow had the second largest increase in accuracy in reducing the amount of misclassified pixels from 32 to 19 (40.6%). This suggests that combining topographic variables is necessary for good discrimination of this class and the digitized NAPP imagery.

Table 19

Error Matrix of the Classification Map Derived from Digitized NAPP Data of Roaring Fork Mountain, Wyoming Combined with DEM Data

Classification	Reference					Row Total	
	MDTM	DM	EF/MV	EF	MTM		
MDTM	57	3	1	0	8	69	
DM	0	4	2	0	0	6	
EF/MV	0	6	71	3	1	81	
EF	0	0	6	31	2	39	
MTM	2	0	2	4	53	61	
Column Total	59	13	82	38	64	216	256
Overall Accuracy = $216 / 256 = 84.38\%$				Khat = 79.2%			

Note. MDTM = Moderately Drained Tundra Meadow; DM = Dry Meadow; EF/MV = Exposed Fellfield/Moist Vegetation;

EF = Exposed Fellfield; MTM = Moist Tundra Meadow.

The addition of the three-variable DEM data set (elevation, slope and incidence) to the digitized NAPP data set increases overall classification accuracy by 6.98%, from 76.17% to 84.38%, and reduces the total error count from 60 pixels to 40 pixels. The addition of the DEM data set appears to significantly increase the classification accuracy.

CHAPTER 5

CONCLUSIONS

The research described in this thesis presents evidence that both the spectral and geomorphic features of an alpine environment can be captured in an integrated data set using high spatial resolution data consisting of digitized NAPP imagery and DEM data. This resolution is only possible, however, at the level of vegetation habitat.

The first objective of this research was to determine the extent to which alpine vegetation types are visible with the spatial and spectral characteristics of a digitized NAPP image. Signature evaluation using the Transformed divergence and Co-spectral plot algorithms suggests that digitized NAPP imagery does not possess the spectral integrity or appropriate bandwidths to distinguish between the subtle differences inherent in alpine vegetation species.

The second objective was to determine if topographic information such as elevation, slope, and aspect derived from field reconnaissance and a USGS DEM would increase the overall classification accuracy when combined with the digital color channels of the digitized NAPP image. There were significant relationships between the surface cover, digitized NAPP, and the topographic variables. I interpret the moderate to high bivariate correlations between the NAPP and topographic variables as evidence that the digitized NAPP image and topographic data sets each contain information that can be used to interpret variations in the surface cover.

An integrated classification using both data sets creates a better set of discriminating variables than either data set alone. Classification accuracies of the field

topographic data and the DEM data that consist of elevation, slope, and incidence are not significantly different from each other. The lack of signature difference between these variables normally indicates that variables taken from a DEM can be substituted for the topographic variables in similar analyses (Jensen, 1996).

Statistical classification using linear discriminant analysis produced overall classification accuracies of 76.17% for the spectral data (digitized NAPP RGB). The classification accuracy of the integrated digitized NAPP and DEM data sets was 84.38%. This is significantly greater than the classification of either data set alone. This result supports the idea reported in the literature, integrating remotely sensed and DEM data in multispectral classifications of mountain environments can increase overall classification accuracy.

In this study, several constraints hampered classification success. Since the digitized NAPP imagery lacked spectral quality the topographic variables were necessary to achieve a high degree of classification success. Though high classification accuracy was achieved using the digitized NAPP image an important consideration in regards to these classification results is only five classes could be distinguished by the digitized NAPP imagery. This significantly increases the chances of identifying correct training classes. The extension of this digitized NAPP technique for regional or global application for classifying alpine vegetation is limited to broad habitat levels and is likely to be complicated by the lack of consistency found between each NAPP image.

Summary and Recommendations for Future Research

Approximately 13,000 square kilometers of alpine environment exists in the western US. These areas are increasingly studied because of their potential sensitivity to global climatic change (Baker, Honaker, & Weisberg, 1995). It has been shown that alpine environments may provide the first warning signs of ecological change as a result of climate change (Walsh, 1987). Management of these fragile alpine environments is of increasing importance, particularly where human activity is present. Alpine environments regulate the flow of water from snow-melt in the alpine regions to semi-arid lowland areas and contain microenvironments that provide valuable habitats for many species of plants and animals. Remote sensing offers a proven and effective method for quantifying and inventorying alpine environments and changes in its vegetation and geomorphic characteristics over time.

Scott's vegetation data were necessary in providing verification of where the vegetation was located in relation to habitat. However, the topographic variables Scott included in his 1970 vegetation survey became the main control for increasing the overall classification accuracy digitized NAPP imagery. Improved classification accuracies and more precise measurements of Scott's vegetation data could be achieved if the methodology were slightly modified using high resolution space and aerial multispectral platforms. Monitoring of the alpine vegetation on Roaring Fork Mountain using the high-altitude AVIRIS platform and the more recently developed high-resolution space-born multispectral IKONOS imagery. These platforms have already proven to be useful in estimating vegetation land cover and could provide more complete and precise spectral

information of Scott's vegetation data. Construction of a micro-digital elevation model (MDEM) in place of the resampled USGS 30 meter DEM used for the Roaring Fork mountain study would probably help to improve the overall classification accuracy and further provide information on the topographic characteristics of Roaring Fork Mountain study area.

REFERENCES

- Baker, W. H., Honaker J. J., & Weisberg P. J. (1995). Using aerial photography and GIS to map the forest-tundra ecotone in Rocky Mountain National Park, Colorado, for global change research. Photogrammetric Engineering and Remote Sensing, 61 (7), 313-320.
- Bamberg, S. A. (1961). Plant ecology of alpine tundra areas in Montana and adjacent Wyoming. Unpublished master's thesis, University of Colorado, Boulder.
- Becking, R. W. (1959). Forestry applications of aerial color photography. Photogrammetric Engineering and Remote Sensing, 25 (5) 559-565.
- Billings, W. D. (1988). Alpine vegetation. In W. D. Billings & M. G. Barbour (Eds.), North American terrestrial vegetation (pp. 391-420). New York: Cambridge University Press.
- Blackstone, D. L. (1993). Geology of Wyoming. In A. W. Snoke, J. R. Steidtmann, & S. M. Roberts (Eds.), Geology of Wyoming: Geological Survey of Wyoming memoir no. 5 (pp. 2-56). Laramie: Wyoming Geological Association.
- Burns, S. F. (1980). Alpine soil distribution and development, Indian Peaks, Colorado Front Range. Unpublished doctoral dissertation, University of Colorado, Boulder.
- Burns, S. F., & Tonkin, P. J. (1982). Soil-geomorphic models and the spatial distribution and development of alpine soils. In C. E. Thorn (Eds.), Space and time in geomorphology: International series no. 12. London: Allen and Unwin.
- Butler, D. R., & Walsh S. J. (1990). Lithologic, structural and topographic influences on snow-avalanche path location, Eastern Glacier National Park, Montana. Annals of the Association of American Geographers, 80 (3), 362-378.

- Caine, T. N. (1969). A model for alpine talus slope development by slush avalanching. Journal of Geology, 77, 92-100.
- Congalton, R. G. (1991). A review of assessing the accuracy of classification of remotely sensed data. Remote Sensing of Environment, 37 (1), 35-46.
- Congalton, R. G., & Green, K. (1998). Assessing the classification accuracy of remotely sensed data: Principles and practices. Boca Raton, FL: CRC/Lewis Publishers.
- Crist, P., & Deitner, R. (May 12, 1998). Assessing land cover map accuracy. Available: <http://www.gap.uidaho.edu/gap/AboutGAP/Handbook/LCA.htm>
- Cybula, W. G., & Nyquist, M. O. (1987). Use of topographic and climatological models in a geographical database to improve Landsat MSS classification for Olympic National Park, Washington. Photogrammetric Engineering and Remote Sensing, 53 (1), 67-75.
- Davis, J. C. (1986). Statistics and data analysis in geology (2nd ed.). New York: John Wiley and Sons.
- ERDAS Field Guide [Computer Software]. (1994). Atlanta, GA: Image Processing Software.
- Evans, I. S. (1972). General geomorphology, derivatives of altitude and descriptive statistics. In R. J. Chorley (Eds.), Spatial analysis in geomorphology (pp. 17-90). London: Methuen.
- Fleming, M. (1988). An integrated approach for automated cover-type mapping of large inaccessible areas in Alaska. Photogrammetric Engineering and Remote Sensing, 54 (5), 1727-1734.

- Frank, T. D. (1988). Mapping dominant vegetation communities in the Colorado Rockies Front Range with Landsat Thematic Mapper and digital terrain data. Photogrammetric Engineering and Remote Sensing, 54 (12), 1727-1734.
- Frank, T. D., & Isard, S. A. (1986). Alpine vegetation classification using high Resolution aerial imagery and topoclimatic index values. Photogrammetric Engineering and Remote Sensing, 52 (3), 381-388.
- Frank, F. D., & Thorn, C. E. (1985). Stratifying alpine tundra for geomorphic studies using digitized aerial imagery. Arctic and Alpine Research, 17 (2), 179-188.
- Franklin, S. E., & Ledrew, E. F. (1984). High relief terrain classification using digital elevation model variables and Landsat MSS data in the Yukon Territory, Canada. Eighteenth International Symposium on Remote Sensing of Environment (pp. 603-611). Paris, France.
- Franklin, S. E., & Moulton, J. E. (1990). Variability and classification of Landsat Thematic Mapper spectral response in Southwest Yukon. Canadian Journal of Remote Sensing, 17 (1), 2-17.
- Franklin S. E., Peddle D. R., Wilson B. A., & Blodgett C. F. (1991). Pixel sampling of remotely sensed digital data. Computers and Geosciences, 17 (6), 775-779.
- Franklin S. E., & Wilson, B. A. (1992). A three stage classifier for remote sensing of mountain environments. Photogrammetric Engineering and Remote Sensing, 58 (4), 449-454.
- Gardner, J. S. (1986). Sediment movement in ephemeral streams on mountain slopes, Canadian Rocky Mountains. In A. D. Abrahams (Ed.), Hillslope processes (pp. 97-113). Winchester, MA: Allen and Unwin.
- Harvie, J., Cihlar, J., & Goodfellow, C. (1982). Surface cover mapping in the Arctic through satellite remote sensing (Report No. 82-1). Ottawa, Canada: Canada Centre for Remote Sensing, Department of Energy, Mines and Resources.

- Hoffer, R., Anuta, P. E., & Phillips T. L. (1972). ADP of multiband and multi-emulsion digitized photos. Photogrammetric Engineering and Remote Sensing, 38 (10), 989-1000.
- Holben, B. N., & Justice, C. O. (1981). An examination of spectral band ratioing to reduce the topographic effect on remotely sensed data. International Journal of Remote Sensing, 2, 115-133.
- Trident Users Guide [Computer Software]. (1998). Hudson, NH: Digital Scanning Software.
- Huberty, C. H. (1994). Applied discriminant analysis. New York: John Wiley and Sons.
- Hutchinson, C. F. (1982). Techniques for combining Landsat data and ancillary data for digital classification improvement. Photogrammetric Engineering and Remote Sensing, 48 (1), 123-130.
- Ives, J. D., & Bovis, M. J. (1978). Natural hazards maps for land use planning, San Juan Mountains, CO. Arctic and Alpine Research, 10, 185-212.
- Jennings, M. D. (May 12,1998). Satellite imagery, pattern delineation and cooperative mapping of land cover. [On-line]. Available: <http://www.gap.uidaho.edu/gap/AboutGAP/Handbook/I.htm>
- Jensen, J. R. (1996). Introductory digital image processing: A remote sensing perspective (2nd ed.). Upper Saddle River, NJ: Prentice Hall.
- Jensen, J. R., & Estes, J. E. (1978). High altitude versus Landsat imagery for digital crop identification. Photogrammetric Engineering and Remote Sensing, 44 (6), 723-733.
- Jensen, J. R., & Toll, D. L. (1982). Detecting residential land use development at the urban fringe. Photogrammetric Engineering and Remote Sensing, 48 (5), 629-643.

- Kenk, E., Sondheim, M., & Yee, B. (1988). Methods of improving the accuracy of Thematic Mapper ground cover classifications. Canadian Journal of Remote Sensing, 14, 17-31.
- Knepper, D. H. (1977). The application of Landsat data to delimitation of avalanche hazards in montane Colorado. Final Report NASA Earth Resources Survey Program. Washington, DC: NASA.
- Kodak Aerial Systems. (1996). Kodak Aerochrome II Infrared Film 2443. (Technical information data sheet No. Ti2161). Rochester, NY: Eastman Kodak Company.
- Light, D. L. (1993). The national aerial photography program as a geographical information system resource. Photogrammetric Engineering and Remote Sensing, 59 (1), 61-65.
- Mace, T. H., & Bonnicksen, T. M. (1982). A comparison of digitized high-altitude photography and Landsat imagery for forest-cover mapping-Apostle Islands, Wisconsin. Journal of Applied Photographic Engineering, 8 (3), 111-116.
- Markon, C. (1992). Land cover mapping of the Upper Kuskokwim resource management area, Alaska, using Landsat and a digital database approach. Canadian Journal of Remote Sensing, 18, 72-72.
- Mausel, P. W., Kamber, W. J., & Lee, J. K. (1990). Optimum band selection for supervised classification of multispectral data. Photogrammetric Engineering and Remote Sensing, 56 (1) 55-60.
- Quirk, B. K., & Scarpace, F. L. (1982). A comparison between aerial photography and Landsat for computer land cover mapping. Photogrammetric Engineering and Remote Sensing, 48 (2), 223-240.
- Scarpace, F. L. (1978). Densitometry on multi-emulsion imagery. Photogrammetric Engineering and Remote Sensing, 44 (10), 1279-1292.

- Scarpace, F. L., Quirk, B. K., Kiefer, R. W., & Wynn, S. L. (1981). Wetland mapping from digitized aerial photography. Photogrammetric Engineering and Remote Sensing, 47 (6), 829-838.
- Scott, R. W. (1970). [Topographic and vegetation field data]. Unpublished raw data.
- Scott, R. W. (1995). The alpine flora of the middle Rocky Mountains: Vol. 1. The middle Rockies. Salt Lake City: University of Utah Press.
- Small, E., & Anderson, E. (1998). Erosion rates of alpine bedrock summit surfaces deduced from in situ 10-Be and 26-Al. Earth and Planetary Science Letters, USA, 150, 413-425.
- Smith, F. (1996). Clustering in Imagine 8.2 for the classification of digital NAPP imagery. ERDAS Users Group Meeting, Atlanta, GA.
- Smith, F., & Pittman, B. (1996). Forest species delineation using digital image processing of scanned NAPP photography. Second International Airborne Remote Sensing Conference and Exhibition, San Francisco, CA.
- Snoke, A. W. (1993). Geologic history of Wyoming within the tectonic framework of the North American Cordillera. In A. W. Snoke, J. R. Steidtmann, & S. M. Roberts, (Eds), Geology of Wyoming: Geological Survey of Wyoming Memoir no. 5 (pp. 2-56). Laramie: Wyoming Geological Association.
- S-PLUS 2000 Guide to Statistics [Computer Software]. (1999). Seattle, WA: Data Analysis Software.
- Steidtmann, J. R., Middleton L. T., & Shuster M. W. (1989). Post-Laramide (Oligocene) uplift in the Wind River Range, Wyoming. Geology, 17, 38-41.

- Tucker, C. J. (1979). Red and photographic infrared linear combinations for monitoring vegetation. Remote Sensing of the Environment, 8 (2), 127-150.
- Turner, B. J., & Thompson, D. N. (1982). Barrier island vegetation mapping using digitized aerial photography. Photogrammetric Engineering and Remote Sensing, 48 (8), 1327-1335.
- Walsh, S. J. (1987). Variability of Landsat MSS spectral response of forests in relation to stand and site characteristics. International Journal of Remote Sensing, 8 (9), 1289-1299.
- Walsh, S. J., Bian, L., Brown, D. J., Butler, D. R., & Malanson, D. P. (1989). Image enhancement of Landsat Thematic Mapper digital data for terrain evaluation, Glacier National Park, Montana, USA. Geocarto International, 4 (3), 55-58.
- Walsh, S. J, Cooper, J. W., Van Essen, I. E., Gallager, K. (1990). Image enhancement Of Landsat Thematic Mapper data and GIS data integration for evaluation and resource characteristics. Photogrammetric Engineering and Remote Sensing, 56 (8), 1135-1141.

APPENDICES

APPENDIX A

NATIONAL AERIAL PHOTOGRAPHY PROGRAM

The National Aerial Photography Program (NAPP) was initiated in 1987 as a replacement for the National High Altitude Aerial Photography program (NHAP). The objective of the NAPP is to acquire and archive photographic coverage of the conterminous United States and Hawaii at 1:40,000 scale, using either black-and-white (B&W) or Kodak color-infrared (CIR) film. The ground resolution is approximately 1 m, depending on the contrast in the terrain. The photographs are acquired by contracting the flying to private industry. These private sector aircraft constitute the NAPP system for photographing the conterminous United States ideally every 5 years. The resulting photographic database is readily available to the public through the EROS Data Center in Sioux Falls, South Dakota, or the Aerial Photography Field Office in Salt Lake City, Utah. The NAPP archive is a national asset, providing photographic coverage for a wide variety of mapping and earth science applications.

The NAPP is designed to acquire photographs at an altitude of 20,000 feet above mean terrain with a standard 6-inch focal length aerial camera using either B&W or CIR film at a nominal scale of 1:40,000. All NAPP flight lines are north-south and provide full stereoscopic coverage with approximately 60% forward overlap and 27% or greater sidelap.

Alternate exposure stations are centered on quarter sections of standard 7.5-minute quadrangles. This positioning of the station is referred to as "quarter-quadrangle centered." Technical specifications for the camera and film in NAPP provide uniform film quality and geometry. The camera's resolution values as tested by the USGS Optical

Science Laboratory must be equal to or greater than 40 p/mm at the lowest area within the camera format and have a geometric distortion of ± 10 m or smaller. The specifications require minimum Sun angle of 30 degrees above the horizon in flat land, and the preferred flying season is generally leaf-off. There are a few exceptions where the vegetation types permit an open flying season. Table 20 shows specific NAPP parameters.

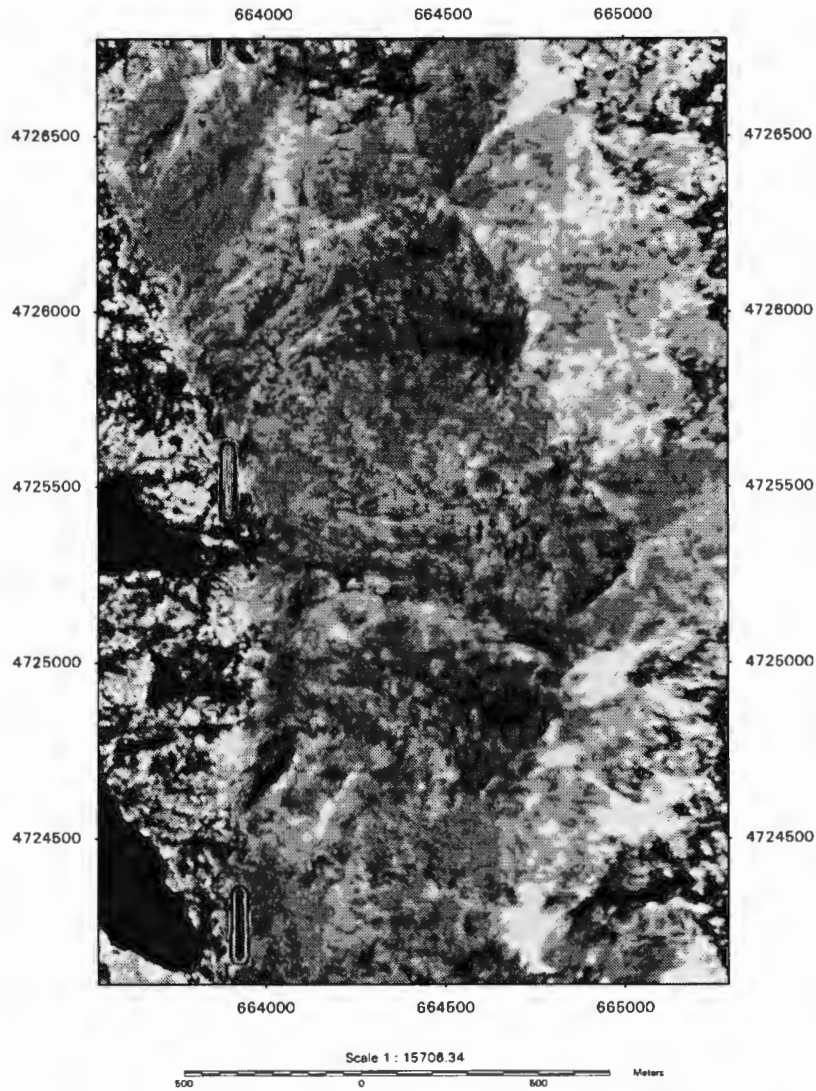
Table 20

NAPP Parameters

Item	English	Metric
Focal length f	6 in	152.4 mm
Format	9 x 9 in	23 x 23 cm
Altitude H	20,000 ft	6,096 m
Coverage/frame	30,000 ft	9,200 m
Exposure spacing B	11,390 ft	3,470 m
B/H ratio	0.57 - 0.60	0.57 - 0.60
Nominal forward lap	60%	60%
Image scale	1:40,000	1:40,000
Film resolution* CIR	686-990 p/in	27-39 p/mm
Film resolution* B&W	838-990 p/in	33-39 p/mm
Stereo photos in 1:24,000-scale quadrangle	0	10
Ground resolution	3.3-4.9 ft	1.0-1.5 m






APPENDIX B

SUPERVISED CLASSIFICATION MAP



Supervised Classification of Alpine Vegetation

Roaring Fork Mountain Study Area
Wyoming, USA

Alpine Vegetation Habitat Classes	
	Moist Tundra Meadow
	Moderately Drained Tundra Meadow
	Dry Meadow
	Exposed Fellfield/Moist Vegetation
	Exposed Fellfield

This map was produced from a digital National Aerial Photographic Program (NAAPP) color-infrared photograph originally acquired on 7-31-89. It was digitized using a Hewlett optical drum scanner at 25 micrometers resulting in 1.02 meter spatial resolution.